uc3m | Universidad Carlos III de Madrid

Systems and Automation Department
Industrial Engineering
Universidad Carlos III de Madrid

Steering Controller for Intelligent Vehicle

Bachelor Thesis

Author: Yekaterina Lertxundi Sesma
Supervisor: Eng. Ahmed Hussein, M.Sc.
Submission Date: 21 June, 2017

uc3m | Universidad Carlos III de Madrid

Systems and Automation Department
Industrial Engineering
Universidad Carlos III de Madrid

Steering Controller for Intelligent Vehicle

Bachelor Thesis

Author: Yekaterina Lertxundi Sesma
Supervisor: Eng. Ahmed Hussein, M.Sc.
Submission Date: 21 June, 2017

This is to certify that:

(i) the thesis comprises only my original work toward the Bachelor Degree

(ii) due acknowledgment has been made in the text to all other material used

---

Yekaterina Lertxundi Sesma
21 June, 2017

Acknowledgments

To my parents, for giving me the chance to receive an education of my choice;
To my friends from University, for being cooperative and not competitive in this experience;
To *Enya*, for making it possible to pull through study nights;
To Pablo Marín Plaza and Ahmed Hussein for helping and guiding me in this Bachelor Thesis.

Abstract

In the last years, the development of autonomous vehicles has arisen a big interest in the big industry of the automotive sector. In addition to several car manufacturing companies, many electronics enterprises are trying to join the market, and a big deal of research is being done in this field. This thesis contributes to said research by developing a steering controller for an autonomous Unmaned Ground Vehicle (UGV).

Due to system specifics, the proposed controller must adapt to the already sealed low-level control of the UGV and function externally to it. The proposed controller is tailored as a deadband compensator, set to overcome the steering motor's internal proportional-integral-derivative (PID)'s steady state error constrains, and prompt the vehicle to respond accurately to the received reference angle. This compensator is created as a C++ code and implemented through Robot Operating System (ROS) architecture.

After the results from the experimental work have been analyzed, the outcome is that the compensator does bring benefit in terms of accurately following the reference steering angle. Qualitative results show that once the compensator is implemented, most of the desired angles are achieved, while only a few cause the system to oscillate. Quantitative results do not present such a favorable outcome, with an improvement of around 9%. This might be due to the result being measured as the mean absolute error instead of the steady state error.

Resumen

En los últimos años, el desarrollo de vehículos autónomos ha generado un gran interés por parte de las grandes empresas del sector automotor. Además de varias compañías de fabricación de coches, muchas empresas de electrónica están intentando entrar al mercado, y se está realizando gran cantidad de investigación en este campo. Este trabajo contribuye a la investigación mediante el desarrollo de un controlador de dirección para un Vehículo Terrestre No Tripulado (UGV) autónomo.

Debido a las particularidades del sistema, el controlador propuesto debe adaptarse al control de bajo nivel preestablecido del UGV, y funcionar externamente al mismo. El controlador propuesto se diseña como un compensador de deadband (zona muerta o zona neutral), establecido para vencer las restricciones del controlador PID interno del motor, e instar al vehículo a responder con exactitud al ángulo de referencia recibido. El compensador es programado en C++ e implementado a través de arquitectura ROS.

Tras analizar los resultados del trabajo experimental, se concluye que el compensador es beneficioso en cuanto a seguir la referencia del ángulo de dirección con exactitud. Los resultados cualitativos muestran que una vez implementado el compensador, la mayoría de los ángulos son alcanzados, y solo unos pocos provocan oscilaciones en el sistema. Los resultados cuantitativos no presentan un resultado tan favorable, con una mejora entorno al 9%. Esto puede ser debido al uso del error absoluto medio como métrica en lugar del error en estado estacionario.

Contents

Acknowledgments **V**

Abstract **VII**

Resumen **IX**

1 Introduction **3**
1.1 Motivation . . . 3
1.2 Objectives . . . 4
1.3 Thesis Structure . . . 5

2 State of the Art **7**
2.1 Drive-by-Wire . . . 7
2.2 Advanced Driver Assistance Systems . . . 7
2.3 Steering Controllers . . . 10
2.3.1 PID Controllers . . . 10
2.3.2 Fuzzy Controllers . . . 10
2.3.3 More Complex Controllers . . . 10

3 Methodology **11**
3.1 Study of the Problem . . . 11
3.2 System Limitations . . . 13
3.3 First Approach: System Modeling and PID Design . . . 14
3.4 Second Approach: Deadband Compensator . . . 16
3.4.1 Current System Behavior . . . 17
3.4.2 Expected System Behavior . . . 18
3.4.3 Algorithm Design . . . 18
3.4.4 Selection of Parameters . . . 20

4 Experimental Work **21**
4.1 Working Platform . . . 21
4.2 Experiments Design . . . 22
4.3 Implementing Code through ROS . . . 25
4.4 Experimental Procedure . . . 25

5 Results **27**
5.1 Behavior without Compensator 27
5.1.1 Scenario 1 27
5.1.2 Scenario 2 30
5.1.3 Concluded Remarks 33
5.2 Behavior with Compensator Version 1 33
5.2.1 Scenario 1 33
5.2.2 Scenario 2 38
5.2.3 Concluded Remarks 41
5.3 Behavior with Compensator Version 2 42
5.3.1 Scenario 1 42
5.3.2 Scenario 2 45
5.3.3 Concluded Remarks 47
5.4 Error Comparison 48

6 Conclusions and Future Work **51**

Appendix **53**

A Lists **54**
List of Abbreviations 54
List of Figures 55
List of Tables 58

B Legislation Framework **59**

C Social Economic Aspect **60**
C.1 Budget 60
C.2 Thesis process 61

D Model **62**

References **66**

Chapter 1

Introduction

1.1 Motivation

It is widely expected that autonomous cars will be a common reality in a not-too-far future from now. So much so, that every major car manufacturing company, as well as many other companies trying to enter the market [1], are investing heavily in research and development for this technology.

The motivation behind this market orientation, beyond the futuristic appeal of it, comes from the reality of deaths caused by traffic accidents. According to the World Health Organization, 1.25 million deaths took place in 2013 just from road traffic. The main cause of said accidents are human errors. Oftentimes, human drivers are faced with situations in which they have a very small amount of time to react and make a decision, and they do not always answer with sufficient velocity, accuracy, or with the right choice. This risk is even bigger in cases of people driving under the influence of alcohol and other substances, bad weather conditions, or even just accumulated tiredness from hours of driving. All of these problems could be fixed by the implementation of autonomous driving.

Although it is true that more and more Advanced Driver Assistance Systems (ADAS) are offered in the market everyday, further research and testing needs to be done before the commercialization of fully autonomous, personal vehicles. It seems natural that autonomous vehicles are just the gradual evolution of driver assistance services, while in reality this transition suffers a considerable disruption. ADAS only work in very specific settings, for a short period of time, whereas in full autonomy a vehicle needs to be able to drive itself continuously for hours, facing all kinds of environments, and without human intervention for correcting. Furthermore, ADAS systems are meant to be used under a driver's supervision, who would correct the movement of the vehicle if necessary, Examples of this are Cruise Control or Assisted Parking. On the contrary, autonomous driving is not supposed to happen under human surveillance, for two reasons: firstly, it should be able to address situations that arise quickly and need an immediate response,

without any time left to warn the driver. Secondly, a further goal of autonomous driving is the disappearance of the driver altogether, in cases where it does not add any value, in terms of production, and only implies a cost (i.e. transportation of goods).

Therefore, autonomous vehicles need to have a full capacity to respond to all possible scenarios in a road - following signs, overtaking, changing lanes, taking an exit, as well as non-foreseeable situations such as a car crash, bicyclist on the edge, or roadwork.

1.2 Objectives

The reliability of autonomous vehicles depends on the system being able to precisely follow the received instructions. If the response of the system is not accurately the desired one, consequences could be terrible. For example, if an automated vehicle's speed is excessively high, it could result on skidding and sliding beyond control, even crashing. Furthermore, if the vehicle is moving at a different velocity than it should, it can miscalculate its current position and make a turn or changes lanes in an inadequate moment, causing an accident. Since avoiding said accidents is the motivation behind vehicle automation, it is essential for the systems to follow the orders they receive with precision. This thesis is focused on the steering of UGVs. Correct and accurate steering is as important as control of velocity, because if done wrongly, it can have the same catastrophic effects. A small difference between the desired angle of the wheels and the actual one creates a big displacement, specially if it is accumulated over time.

The aim of this work is to study the current performance of the steering system on an UGV, and develop a controller to achieve a precise and correct response regarding the steering angle of the wheels. This angle can be defined as that between the front of the vehicle and the direction it follows. Figure 1.1 ilustrates this concept.

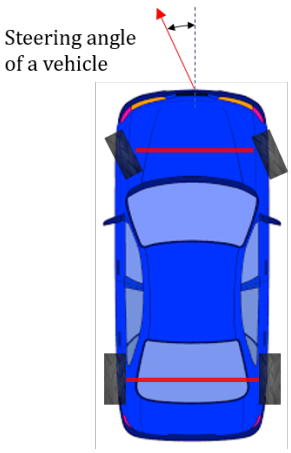

Figure 1.1: Steering angle of a turning vehicle

1.3 Thesis Structure

This thesis is structured as follows:

Chapter 2 is comprised by an overview of the state of the art regarding ADAS. It introduces the path from classical vehicles to autonomous ones, going into the development of ADAS through time, and finally it presents several approaches utilized on different papers for controlling the steering.

Chapter 3 carries out two different approaches to the problem of steering, and it introduces some of the vehicle specifics that limit and define these approaches. After discarding one of the methods, a controller is developed by means of the other one.

Chapter 4 presents the testing environment and develops the experimental procedure for implementing and testing the designed controller.

Chapter 5 analyzes the outcome of the experiments, draws conclusions and develops a new version of the controller based on said conclusions.

Chapter 6 summarizes the outcome of this thesis and suggests future research based on it.

Chapter 2

State of the Art

2.1 Drive-by-Wire

The first step in the transition from classical, purely mechanical vehicles to autonomous vehicles is the substitution of the mechanical linkages (steering column, intermediate shafts, belts, coolers...) by electrical or electro-mechanical systems, as can be seen in Figure 2.1, further explained in detail in [2]. This system, at which the vehicle is not autonomous yet, but control and electronics are involved, is known as Drive-by-Wire or X-by-Wire. Depending on which area of the driving process is being electronically controlled, this technology can also be called Throttle-by-Wire, Brake-by-Wire, Steer-by-Wire or even Park-by-Wire. Further examples of these systems are explained later on.

Drive-by-Wire has drawn considerable attention of engineers and researchers in the area of vehicle dynamics and control since the mid of 1980s. According to [3], this is due to the improved steering performance and increased passengers' safety and comfort they provide. As a matter of fact, according to [4], *"studies have shown that dynamic driving controls are the second most efficient safety system for passengers, outmatched only by the seatbelt (Aga et al. 2003, Sferco et al. 2001)"* However, while the conventional proportional-derivative control is acceptable, the design of a robust controller for Drive-by-Wire systems results challenging. A possible resolution can be found in [3].

On the other hand, the increased social concern regarding traffic [5], has created interest and favored research in autonomous vehicles. In [6], the functions of these vehicles are classified into two main aspects: assistant driving and automatic driving. The former is devoted to improving safety and riding comfort, and is materialized by the emergence of ADAS.

2.2 Advanced Driver Assistance Systems

The ADAS technology is increasingly available on the market. It started on the late 70s and kept expanding. However, it is far from being a fully exploited field. Nowadays, some

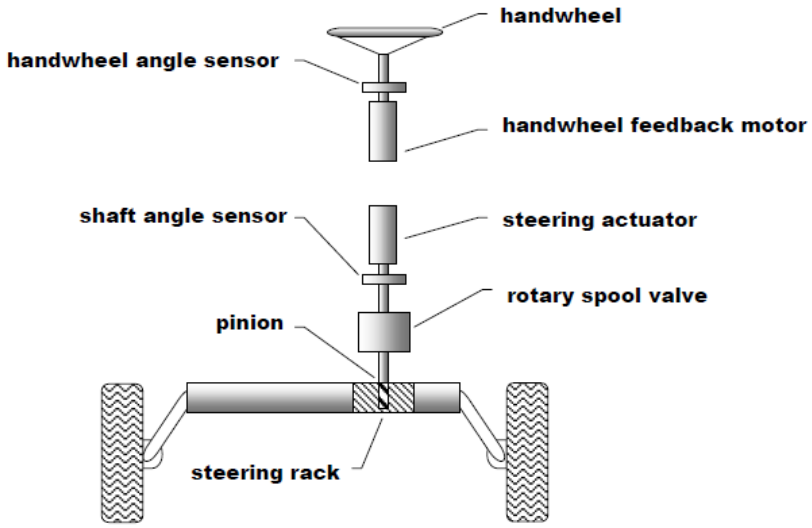

Figure 2.1: Example of the substitution of classically mechanical linkages for an electronic system on Steer-by-Wire [2]

ADASs are a common feature in every car, to the point where some of them are mandatory by law (e.g. Antiblock Brake Systems (ABSs) are required on all new passenger cars sold in EU since 1st July 2004) [7], while others are considered an "extra accessory" (e.g. the rear view camera on parking assistance). Figure 2.2 shows the evolution of Drive-by-Wire, from the first ADASs towards full automation.

According to the extensive review of ADASs done in [4], the first of these systems were proprioceptive, which means that they registered information regarding the internal status of the vehicle. Therefore, the control they exert mostly concerns vehicle dynamics. An example of this kind would be the already mentioned ABS, which serves the purpose of avoiding a vehicle's tires sliding out of control, by varying the braking force. Later on, a Traction Control System enhanced the original one. A few years later Electronic Stability Control was developed: this system, which centralizes ABS and traction control, has the aim of avoiding skidding, understeering and oversteering.

Due to technological advancements, the use of exteroceptive sensors started. These sensors provide information of the surroundings of the vehicle, and are mostly used on informing and warning the driver, as well as increasing comfort. One of their main applications is the assistance with navigation: following the optimal route brings benefits regarding safety, pollution and time and fuel efficiency.

Parking assistance (Park-by-Wire) entered the market at the hand of ultrasonic sensors. They have evolved from a mere warning system, that helps avoid collisions while parking, to the incorporation of a rear view camera showing the driver precisely the location of the obstacles around, to vehicles fully capable of autonomously parking on a spot selected by the driver.

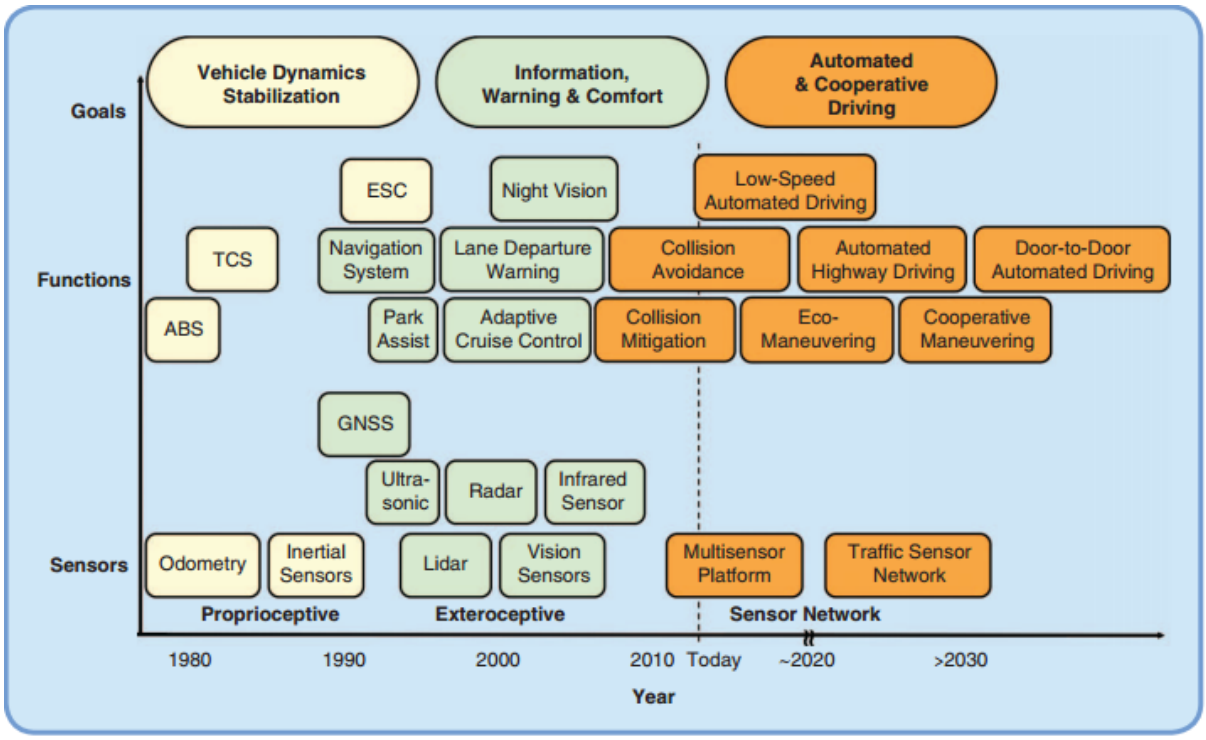

Figure 2.2: Past and potential future evolution [4]

An assistance system that implements Throttle-by-Wire is Adaptive Cruise Control. This feature enhances safety as well as driver's comfort, because it is able of keeping a stable velocity, adjusting it at the presence of other vehicles ahead, keeping an adequate distance. Therefore, traffic flow is improved as well.

Forward collision prevention systems are currently being marketed for low speeds. This feature bring a positive economical impact, by avoiding vehicle damage. Similarly, long range collision mitigation serves the same purpose. Even if the collision is not completely avoided, damage is taken to a minimum. This proves specially favorable for trucks and vehicles with low maneuverability, for the earlier braking they require.

Lane Departure Warning System, as well as its evolution of Active Lane Keeping Assistance address the main cause of accidents, which is unwanted and uncontrolled change of lanes, due to drivers' lack of attention. The downside of this systems is that, although useful, they rely on visible lane marks, and cannot work on unmarked roads.

In summary, a wide range of ADASs are offered in the market nowadays. In the majority of the presented techniques, although control circuits are implemented, the decision-making process is ultimately, human, and therefore cannot be considered autonomous. However, this technological advancements offer the necessary basis for further development until full automation, where all the already considered scenarios, the in-between ones and unexpected situations that may arise will be addressed satisfactorily without human intervention.

2.3 Steering Controllers

Since the main focus of this thesis is the control of the steering of an UGV, the following section presents the different approaches and techniques found on the literature seeking to solve this same problem.

2.3.1 PID Controllers

In [8], a PID controller is implemented, and the proportional, integral and derivative gains are experimentally determined. However, there is a dead band, within a range of -6% to 6% of torque where the motor torque is too small to influence the steering handle. In order to fix this, a dead-band compensator is introduced. In doing so, time delay and lateral error are reduced.

In [9], a robust PID steering control is developed using the Parameter Space approach. The designed controller performs satisfactorily in later simulations.

2.3.2 Fuzzy Controllers

Fuzzy logic controllers are used in [6] and [10], due to the similarity with a human driver's behavior. It is necessary to point out that in neither case was the fuzzy controller the only system managing the steering. In [6], a backstepping equivalent control law and a fuzzy sliding mode reaching control law are constructed, specially aimed at the coupled and nonlinear features of autonomous vehicles in the conditions of emergency obstacle avoidance, whereas in [10], a cascade control architecture is implemented, closing with an external fuzzy control loop. This way, the control architecture gives good results for different vehicle speeds and curves. The PID controller implemented in the inner control loop smoothes out any sudden changes in the fuzzy control output signals, which is particularly important at low speeds.

2.3.3 More Complex Controllers

An H_∞ control strategy is developed in [11]. The desired trajectory of the vehicle is considered already known, and the obtained closed loop performance is studied in vehicle trajectory following. The proposed controller performs very well in trajectory tracking.

A nonlinear Model Predictive Control (MPC) is the method of choice in [12]. MPC is of systematically handling model non linearities, uncertainties and constraints. Its ability to predict future steps distinguishes itself from other advanced control schemes. However, the linearization about an operating point that is commonly done is not suitable for systems such as autonomous vehicles, due to their strong nonlinearities causing said linearized approaches only to apply to low curvature roads. On the other hand, usual nonlinear MPCs require a huge computation power. That is why in [12], a tailored algorithm is designed.

Chapter 3

Methodology

3.1 Study of the Problem

The used UGV for the experimental work in this thesis has a steering control algorithm, but it does not show satisfactory results [13]. Figure 3.1 portrays the comparison of the odometry from the Velodyne, a very accurate lidar sensor, and the data from the wheel encoders odometry. Odometry is defined as the estimation of position, over time, based on data collected from sensors.

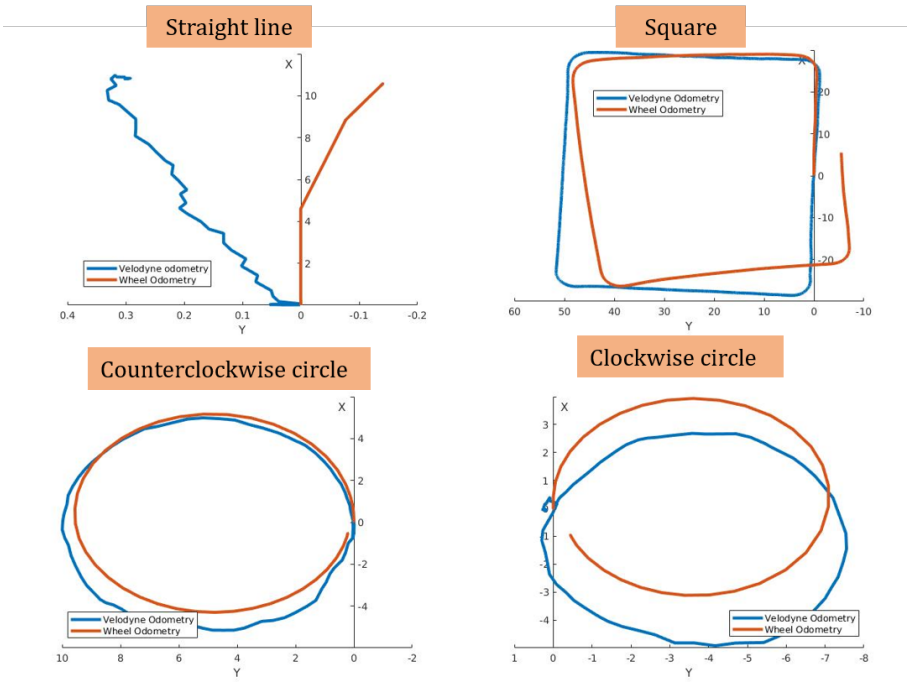

Figure 3.1: Comparison of Velodyne and wheel encoder odometries on different path geometries

Taking the data from the Velodyne (blue line) as the true displacement, due to its high accuracy, it is possible to observe that the information that the wheels odometry provides (red line) does not match reality. For example, focusing on the top left image in Figure 3.1, it is possible to see that when the data from the wheels odometry shows the UGV moving on a straight line, in reality that is not true. Therefore, the computation of the odometry from the wheels is wrongly done. This might be due to various reasons:

- The model used for the calculations is wrong.
- The reading of the wheels' steering angle is wrong, therefore the calculations are performed with wrong data.
- The system is unable of following the received orders properly, and when it is told by the steering controller to move the wheels to a specific angle, it falls short or long. However, it computes the odometry using the angle values that it should reach instead of the ones it actually achieves.

Regarding the first option, the model used for the calculation is the bicycle reduction of the Ackerman model, as explained in [13]. The use of this model is widely accepted in the automotive industry. As stated in [13], having the vehicle's current position and next waypoint position (with respect to the vehicle position, noted as X_g and Y_g on polar coordinates) as inputs, the Covered Distance (CD) is evaluated with equation 3.1.

$$CD = \sqrt{X_g^2 + Y_g^2} \tag{3.1}$$

Vehicle curvature (VC) is calculated with equation 3.2, which is derived from the Ackerman model of Pure Pursuit algorithm. VC is inversely proportional with the vehicle radius of rotation (R), as shown in equation 3.3.

$$VC = \frac{2 \cdot X_g}{CD^2} \tag{3.2}$$

$$R = \frac{1}{VC} \tag{3.3}$$

The vehicle reduced to bicycle Ackerman model as seen in Figure 3.2. Equation 3.4 is used to calculate the necessary steering angle *theta* for the vehicle to reach the goal position, where (L) is the vehicle's length from axle to axle, COR is the center of rotation and (COM) is the vehicle's center of mass.

$$\tan(\theta) = \sqrt{\frac{LWB^2}{R^2 - COM^2}} \tag{3.4}$$

The other two hypothesis as to why the steering is not working properly, having erroneous readings and not being able to follow the path planner's orders are going to be used as the initial point for tailoring a solution to the problem in this thesis.

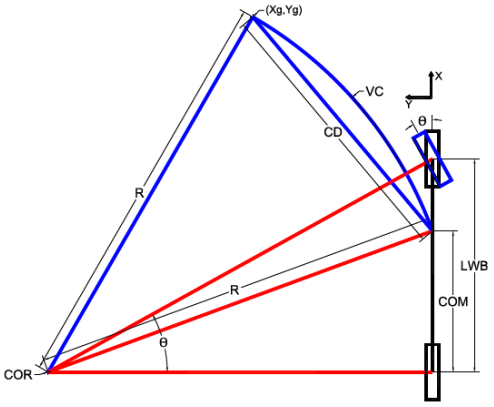

Figure 3.2: Graphical model for wheel odometry [13]

3.2 System Limitations

In order to be able to design an appropriate controller for an UGV, it is necessary to take into account the specifics of the system. In this case, the only aim is to control the steering of the wheels, and the rest of parameters regarding the movement of the vehicle are assumed to be taken care of (control of speed, braking, etc.). One particularity of the vehicle available for the testing of this thesis is that part of its steering control architecture is already determined. More specifically, the low level control of the vehicle has a PID controller that cannot be modified. Figure 3.3 presents an scheme of the architecture regarding the steering control of the UGV.

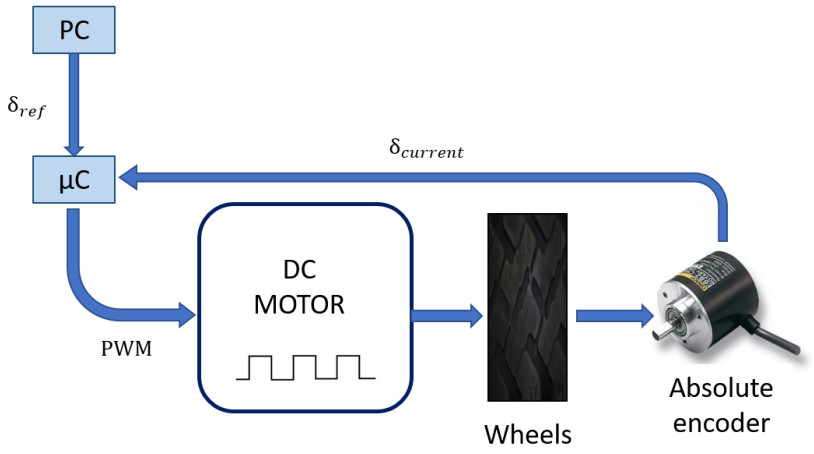

Figure 3.3: Control architecture on UGV

The functioning is as follows: The computer sends an order of the steering angle

that the wheels should reach, the reference angle (δ_{ref}). Then, a micro-controller sets a PWM to send to a DC motor. The motor moves the wheels, and said displacement is measured by an absolute encoder. This measurement is feedbacked to the micro-controller, informing of the current angle ($\delta_{current}$) of the wheels. The micro-controller contains a PID controller [13]. All of this comprises the low-level control of the steering, and its representation as a diagram can be seen in Figure 3.4

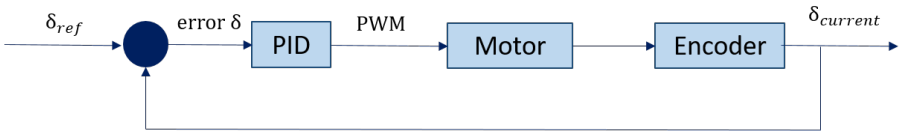

Figure 3.4: Original control scheme on UGV

3.3 First Approach: System Modeling and PID Design

The first approach to solving the problem is based on the hypothesis that the readings of the steering angle are wrong. That is, that the correlation between the reading of the encoder and the $\delta_{current}$ is erroneous. Based on the success of a PID controller seen in [8], and [9], it is intended to model the system to find the correct relation, and afterwards design another PID for the problem at hand in this thesis. As stated before, in this particular case it is not possible to access or modify the low level control. Therefore this thesis will approach the issue of control externally from it. An external control scheme is proposed, as seen in Figure 3.5

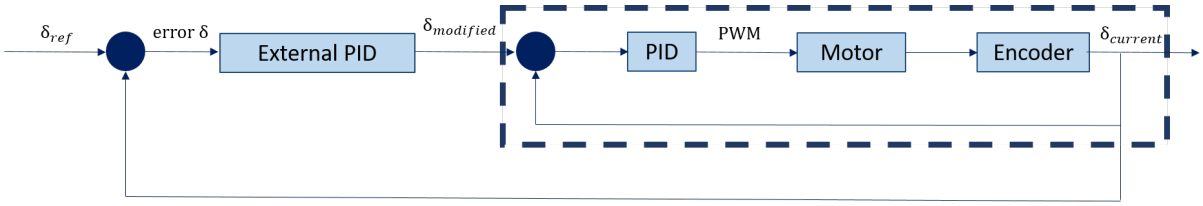

Figure 3.5: Proposed control scheme on UGV

The steering geometry of a UGV is assumed to correspond to the Ackerman model, as stated on Section 3.1. This model, invented by the German carriage builder Georg Lankensperger in Munich in 1817 [14], still stands today. The name of the model comes from Lakensperger's agent, Rudolph Ackermann, who patented it. The model defines the turning geometry of vehicles in the way shown in Figure 3.6.

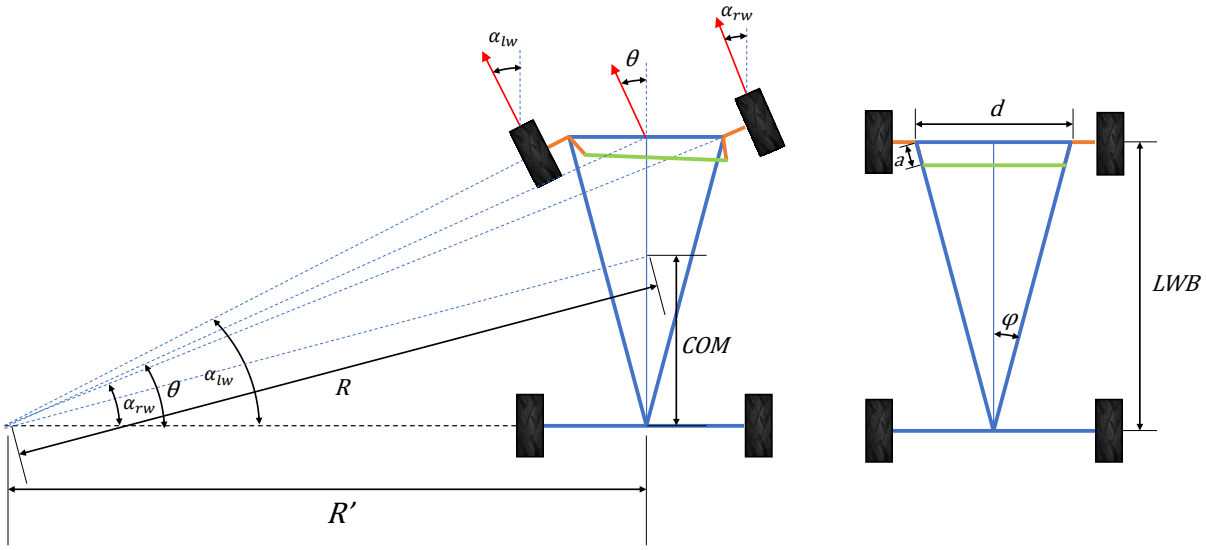

Figure 3.6: Ackerman model

The particularity of this geometry is that when turning, imaginary lines perpendicular to each wheel coincide on the center of rotation. Consequently, the angle of each front wheel coincides with the angle between a line perpendicular to the center of the wheel and a line perpendicular to the rear wheels. It is possible to deduce the equations that correspond to this system. Figures 3.6 portrays the nomenclature for the dimensions of the drawing. Table 3.1 explains the meaning of each dimension.

Table 3.1: Nomenclature of dimensions

Name	**Meaning**
φ	Ackerman geometry angle
θ	Steering angle of vehicle
LWB	Length of main axis
COM	Position of Center of Mass
α_{rw}	Right wheel angle
α_{lw}	Left wheel angle
d	Length of front axle, joint to joint
R'	Distance from COR to main axis
R	Radius of turn

Set of equations from the model:

$$\varphi = \arctan\left(\frac{d/2}{LWB}\right) \tag{3.5}$$

$$\theta = \arctan\left(\frac{LWB}{R'}\right) \tag{3.6}$$

$$\alpha_{rw} = \arctan\left(\frac{LWB}{R' + \frac{d}{2}}\right) \tag{3.7}$$

$$\alpha_{lw} = \arctan\left(\frac{LWB}{R' - \frac{d}{2}}\right) \tag{3.8}$$

$$R' = \sqrt{R^2 - COM^2} \tag{3.9}$$

The objective is to mathematically relate the position of the encoder, that measures how much the motor has turned, to the movement that said turn produces on the mechanical shafts of the UGV. Then, the movement on the mechanical shafts must be related to the steering angle of the vehicle.

The mathematical model of the relation between the steering angle of the vehicle and the movement of the mechanical shafts can be found in Appendix D. The model of the motor-encoder relation is simply that of an electrical DC motor. However, this approach has been discarded and not further developed due to the difficulty to establish the relation between the motor and the shafts movement. After inspecting the mechanical links of the UGV, it was seen that the mechanism was not as simple as the graphical Ackerman model may depict (this does not mean that the model does not hold in regards of turning; it only implies that the real structure of the vehicle is not that of the simple sketch). Due to the complexity of the mechanism, and specially the difficulty for taking measurements of dimensions of any type, this approach was abandoned.

3.4 Second Approach: Deadband Compensator

After the lack of success of a general system modeling and PID design classical approach, another look was taken to the problem at hand. As mentioned earlier, the UGV at hand for testing has an internal PID that cannot be modified. The steady state error of this PID is set to a value of $\pm 0.3°$, which means that when the current steering angle is within that range with respect to the reference angle, the motor will stop [13]. This constrain creates a deadband of $\pm 0.3°$. The idea of this new approach is to compensate for the deadband, in which the motor is constrained from moving. The proposed control scheme is the one shown in Figure 3.7

Therefore, this compensator receives a desired steering angle as an input from the on-board computer, performs the necessary operations, and provides a modified reference

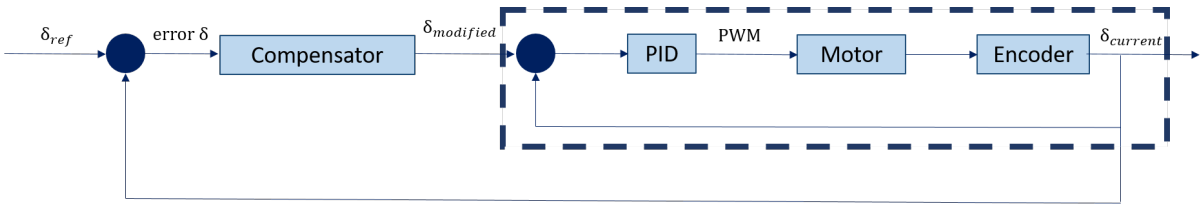

Figure 3.7: Control scheme including compensator

as an output, which is introduced to the micro-controller embedded on the vehicle. The compensator is written as a C++ code, and it is implemented to the UGV through ROS architecture.

3.4.1 Current System Behavior

Due to the manually developed internal PID controller responsible for the steering, the correct output angle is not always achieved, and instead of being the desired one it lies within a $\pm 0.3°$ range of the reference. Figure 3.8 portrays a few possible scenarios of varying error.

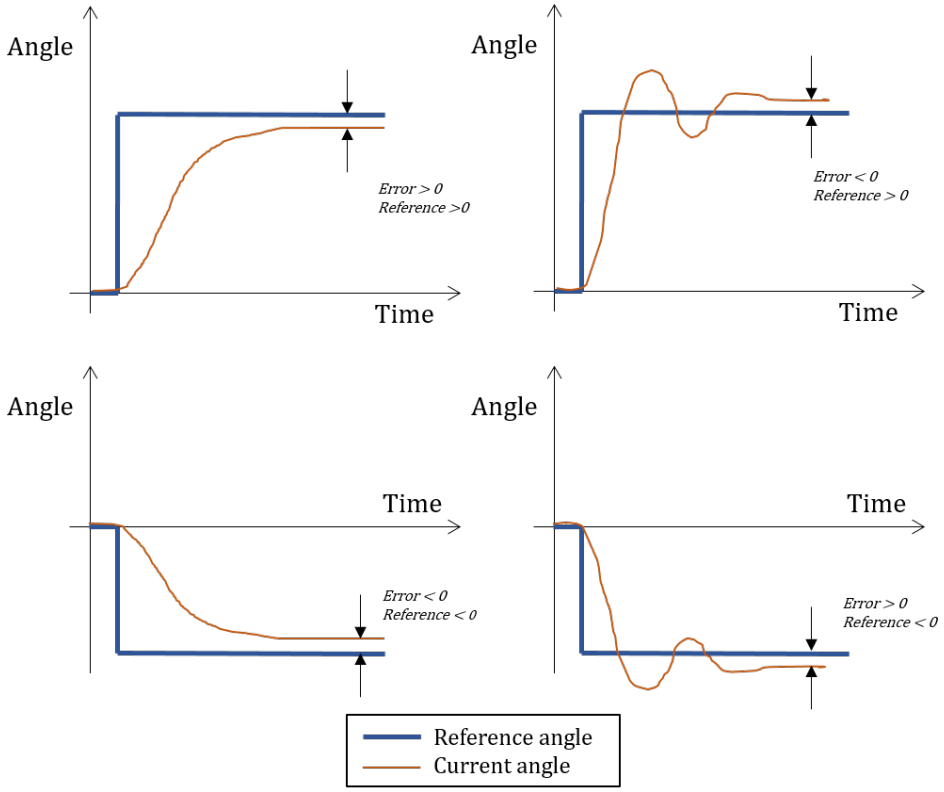

Figure 3.8: Position error explanation

3.4.2 Expected System Behavior

The goal of the compensator is to provide a modified reference, thus the vehicle is able to reach the desired steering angle. This is represented in Figure 3.9: when the system starts to stabilize on a value that is not the desired one (pointed by the arrow), a modified reference will be provided to the system. Once again, the system will be unable to reach it, but on trying it will arrive to the reference angle that is, ultimately, the desired one.

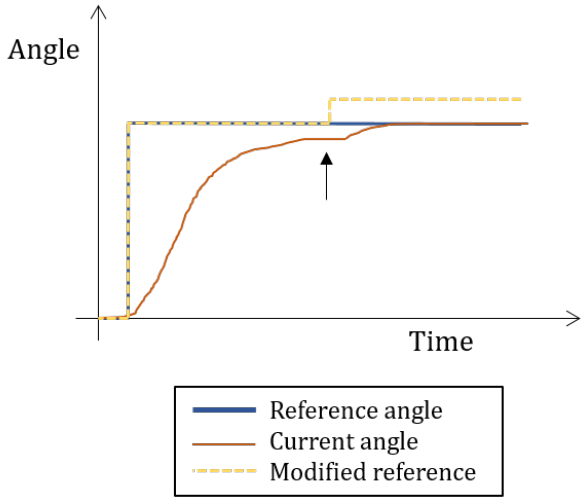

Figure 3.9: Expected behavior after implementing the compensator

3.4.3 Algorithm Design

Figure 3.10 presents the algorithm of the compensator. First, the current angle of the wheels and the reference (desired) angle are registered. Afterwards, it is necessary to check if the system has stabilized, because it does not make sense to provide a modified reference if the wheels are still in transition and far from the desired angle. In order to check stability, the variation of a specific amount of current angle readings is computed. If it exceeds an specific threshold, the system is deemed unstable and the modified reference is the same as the original reference. However, if the system is stable, the error is computed.

$$Error = \delta_{reference} - \delta_{current} \tag{3.10}$$

If the error equals zero, the system already reached the desired angle. However, if this is not the case, a modified reference must be provided. This modified reference is computed by adding or subtracting a fixed value from the original reference, depending on the sign of the error being positive or negative, respectively.

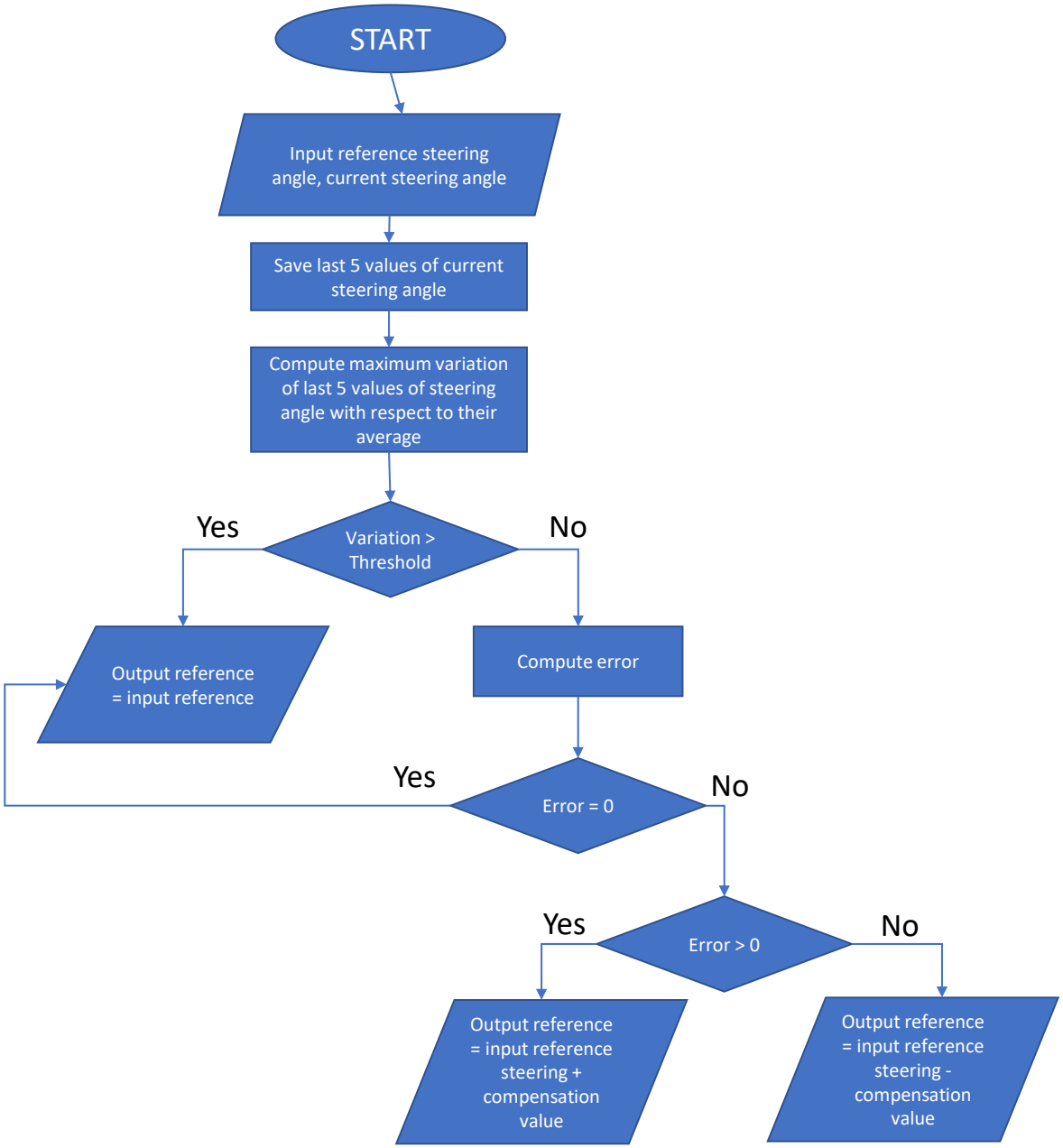

Figure 3.10: Algorithm of the compensator

3.4.4 Selection of Parameters

Table 3.2 collects the parameters selected for the compensator, as well as their justification.

Table 3.2: Selection of parameters for the compensator

Parameter	**Value**	**Reason**
Number of readings taken into account for stability calculation	5	If the number is too high, the system will respond slowly. However, if it is too low, it might deem as stable some scenarios that are not. In order to avoid that, and taking into account a sample frequency of 20Hz, this is the selected amount.
Threshold of variation allowed for considering the system stabilized	0.05°	Acceptable error. If the threshold is too high, the system might not be actually stable when the program deems it so. If it is too low, small external disturbances might induce a variation enough to exceed this threshold, and the system will never be considered stable, even if it is.
Fixed value added/subtracted to the reference angle in order to obtain the modified reference	0.3°	That is the range set to protect the DC motor. If the current steering is at a greater distance than this set value, it should be enough to make the motor move. A lower value might not get the motor moving, while a higher one might create an oscillation.

Chapter 4

Experimental Work

4.1 Working Platform

Figure 4.1: The testing vehicle, iCab1

The platform, for which the compensator has been designed, is an electric golf cart, commercialized under the name of E-Z-Go. Several modifications have been performed on this vehicle, with the aim of conditioning it to become an autonomous vehicle. The cart, see Figure 4.1, is used by the Laboratorio de Sistemas Inteligentes (LSI) as a research platform, and it has been named iCab.

Modifications that concern the steering are: substitution of the steering wheel by a motor-encoder system, to control the direction electronically, as portrayed in Figure 4.2. Additionally, the throttle paddle is deactivated and the traction electric motor of forward and backward motion is controlled by means of a power amplifier circuit. Regarding perception of the surroundings, cameras and sensors have been installed: a laser rangefinder and a stereo vision binocular camera. These are connected to an on-board embedded computer.

Figure 4.2: Motor-encoder system on iCab1

4.2 Experiments Design

The goal of the experiments is to know how the vehicle behaves before implementing the compensator and how it behaves once the compensator is implemented. In order to have comparable data from both of these situations, it is necessary to create a repeatable scenario to subject the vehicle to. In other words, the UGV must receive exactly the same inputs, repeatedly, to see how it responds differently depending on the presence or absence of the compensator.

In this case, the **inputs** are **reference angles** that the vehicle's steering must achieve and the **output** is the **current steering angle** of the vehicle, which will show whether the UGV has reached the desired angle or not. As stated before, the inputs need to be repeatable, reproducing exactly the same scenario. Usually, the input reference angle comes from the movement manager ROS-node, if the vehicle is driving on autonomous mode, or from a joystick hand control if the vehicle is moving manually. But neither of these methods is adequate for the experiments, because they do not assure equal conditions in all the experiments. For example, on manual mode, even if the same references are sent on the same order, due to human intervention it cannot be guaranteed that the timing (in this case, the separation between each reference angle) will be exactly the same on every experiment.

To address this problem, a simple code is developed. This code generates the messages with the reference angles at the designated times, and it is executed on every experiment. This guarantees equal conditions on the system's input, which implies that the outputs can be compared on a meaningful way.

The task of choosing the angles that will be a reference during the experiments is not trivial. It is desirable to obtain information about the response of the vehicle on different regions (angles), because the behavior changes when the wheels are steering close to the center in comparison with further to the laterals. Additionally, it is intended to study how the system responds to a variety of jumps: what happens when the difference (in

degrees) from one reference to the next one is just slight, medium or abrupt. Figure 4.3 depicts the sign convention for angles used in this thesis.

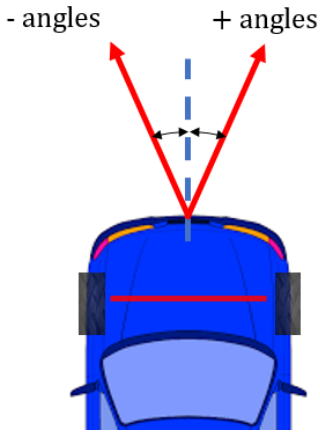

Figure 4.3: Sign convention of steering angles

Taking all of this into account, a list of reference angles is designed. To inspect the system's behavior on different regions of the turning range, different positions are selected (e.g. 10°, -5°...), and then the reference moves around it. This way it is possible to know the behavior of slight changes on different regions. To also characterize the vehicle's response to bigger shifts, medium and abrupt reference changes are inserted in between. Figure 4.4 presents the sequence of angles chosen for the experiments. Due to practical reasons (lack of space for the testing UGV to move), the whole list of angles that are to be tested is split in two, named Scenario 1 and Scenario 2. However, the experiments were carried out in both scenarios.

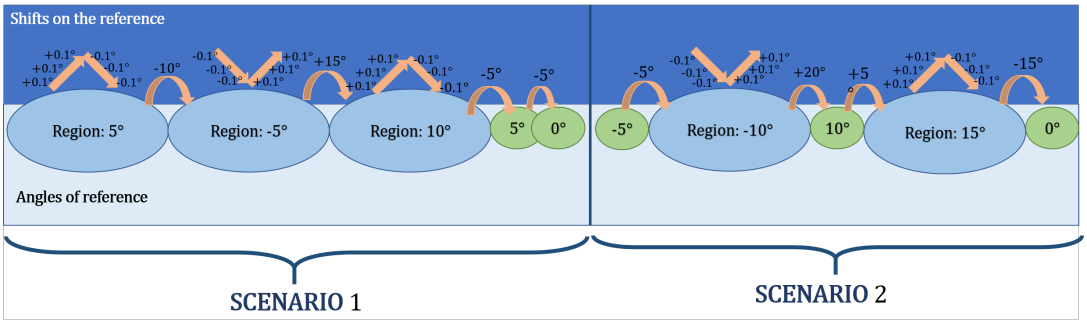

Figure 4.4: Reference angle sequence for the experiments

Regarding time, the code that sends the messages with the reference angles to the vehicle also takes care of doing it on a specific timing. The amount of time that a reference is set depends on the jump there has been to arrive to it. For example, if the first reference is set on 5°, and the second one on 10°, the second reference will be allowed a longer time

Table 4.1: List of angles and durations on each scenario

Scenario 1				**Scenario 2**			
Angle(°)	Time (s)	Angle(°)	Time (s)	Angle(°)	Time(s)	Angle(°)	Time (s)
5	5	-5.1	2	-5.0	5	15.3	2
5.1	2	-5.0	2	-10.0	5	15.2	2
5.2	2	10.0	5	-10.1	2	15.1	2
5.3	2	10.1	2	-10.2	2	15.0	2
5.2	2	10.2	2	-10.3	2	0.0	5
5.1	2	10.3	2	-10.2	2	Total	49
5.0	2	10.2	2	-10.1	2		
-5.0	5	10.1	2	-10.0	2		
-5.1	2	10.0	2	10.0	5		
-5.2	2	5.0	5	15.0	5		
-5.3	2	0.0	5	15.1	2		
-5.2	2	Total	61	15.2	2		

to stabilize than if the second reference had been 5.1°. This is due to the fact that for bigger jumps, the system usually overshoots and takes longer time to stabilize. In this experiment's design, however, the timings have been kept simple: any shift considered "slight change" (less than 0.5°) has 2s of the current reference value set, before the next reference is sent in; whereas any shift considered medium (5° or above) or abrupt (10° or above) has a 5s time of set, before receiving the next reference. Table 4.1 presents the final design of the experiment: for each scenario, what the list of references is going to be, each reference paired with the amount of time it will be held.

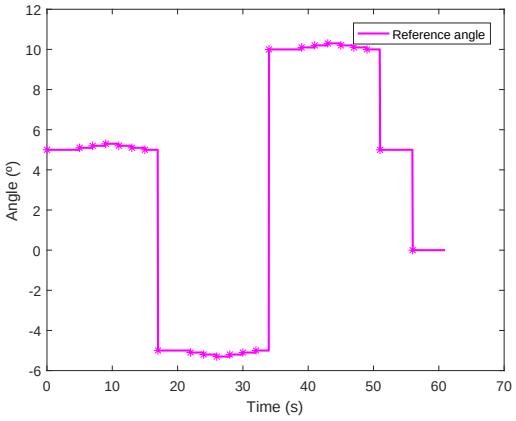

Figure 4.5: Scenario 1: plot of reference angles

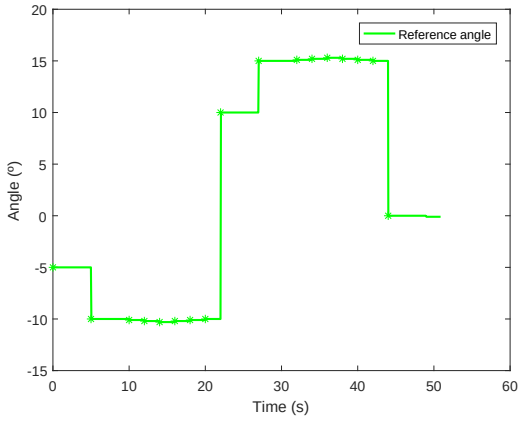

Figure 4.6: Scenario 2: plot of reference angles

Figures 4.5 and 4.6 present the plot of angle of reference versus time, for Scenario 1

and Scenario 2 respectively. This means that those graphs are the reference the system will try to follow. The asterisk have been added to make the transition from one value to the next one more clear.

4.3 Implementing Code through ROS

Once the C++ code is debugged and ready for implementation, it must be embedded in ROS-based architecture. The program is implemented as a ROS-node, which subscribes to the messages sent by the *reactive_tasks* node, and publishes messages through the output of *movement_manager*. In this manner, the program receives the steering reference angle (δ_{ref}), performs the necessary computation, and returns a modified reference ($\delta_{modified}$) as an output. The latter is the command that the UGV follows.

4.4 Experimental Procedure

First, the vehicle must be prepared for the experimentation. The battery must be charged, the program of the compensator must be embedded on the architecture, and the code with the references commands must be ready to be executed. The vehicle is taken to an appropriate location with enough room to complete the displacement commanded by the code.

Then the experiments can begin. The procedure during each experiment consists on executing the code containing the list of reference angles, while recording the relevant data of the UGV's response: current steering angle, reference steering angle and modified reference, when applicable. This has to be done both before and after implementing the controller, to find out the change of behavior that the compensator causes. More specifically, the experiments have been run in this order:

- Run Scenario 1, **without** implementation of the compensator. This is done twice, Experiment 1 and Experiment 2.
- Run Scenario 2, **without** implementation of the compensator. This is done twice, Experiment 3 and Experiment 4.
- Run Scenario 1, **with** implementation of the compensator. This is done twice, Experiment 5 and Experiment 6.
- Run Scenario 2, **with** implementation of the compensator. This is done twice, Experiment 7 and Experiment 8.

Chapter 5

Results

5.1 Behavior without Compensator

This section presents the response of the system to both experiment scenarios before the implementation of the compensator. Two experiments were made, and both of them are displayed because the system did not behave exactly the same on both.

5.1.1 Scenario 1

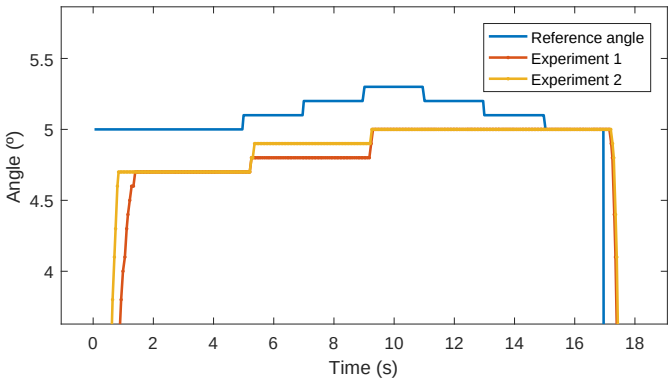

Figure 5.1: Response around 5°

Figure 5.1 presents the beginning of the trial, where the aim is to study the behavior of the system, both under slight and abrupt turns, on the area around the 5° angle. The vehicle starts with an steering angle of 0°, and the first reference (blue line), starting at t=0s. is 5°, which none of the experiments achieved, stabilizing at 4.7°. Following, the reference goes through several slight increases, to which the system responds with a small

delay(of around 0.25s), but it is still unable to reach the desired angle. Experiment 1 the error increases to as much as 0.4°, which lays outside the motor's protection deadband. When the reference starts to decrease, the steering angle of the vehicle stays the same because the reference is still higher than the output.

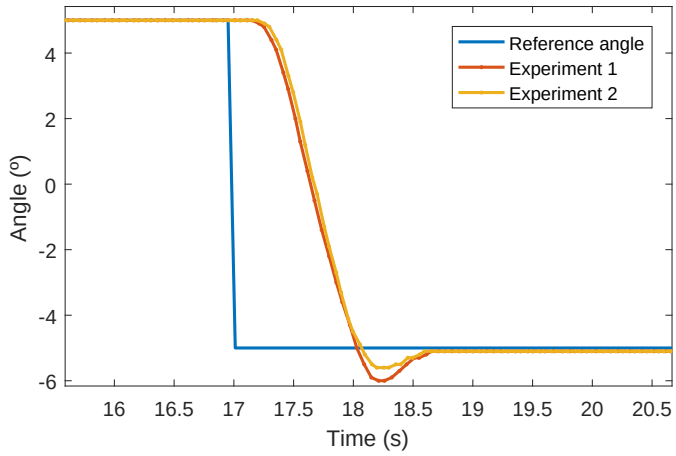

Figure 5.2: Drop from 5° to -5°

In Figure 5.2, an abrupt drop from 5° to -5° is represented. In this case, due to inertia, the turn, the wheels go to an angle further than intended. This is called an overshoot. However, when trying to return to the reference angle, the system is unable to reach it, and it stabilizes with an error of 0.1°

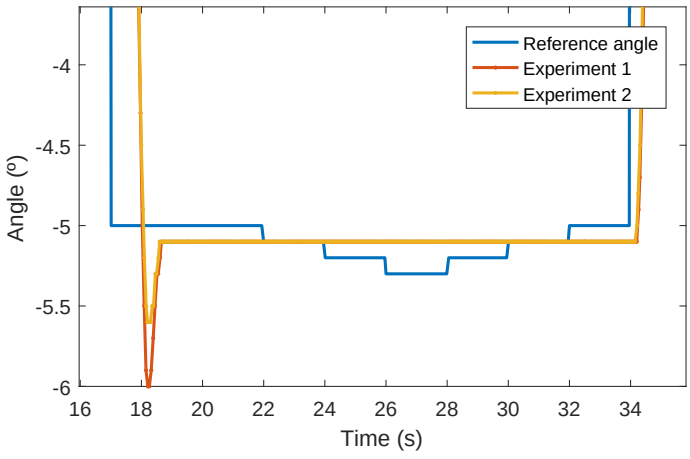

Figure 5.3: Response around -5°

Figure 5.3 shows how after the overshoot and stabilizing at an erroneous value, the reference angle goes through a slight decrease followed by slight increase process, during

all of which, on both experiments, the system does not move to either direction. The maximum error is of 0.2°, and since it lies within ±0.3° of the reference, this fulfills the expectations.

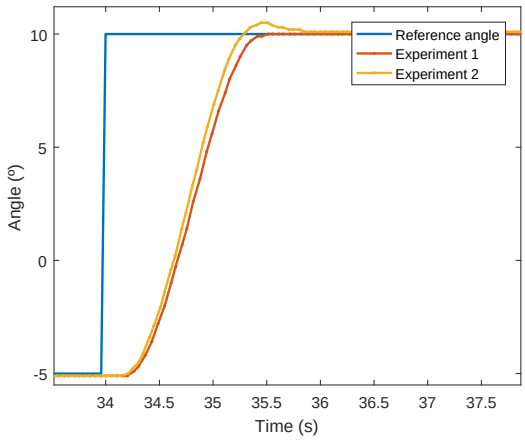

Figure 5.4: Jump from -5° to 10°

Figure 5.4 portrays a specially abrupt increase on the reference. In this case, one of the experiments is successful at achieving the desired angle, with no overshoot at all, while the other one overshoots up to 0.5° above the reference, and does not manage to return to it. This can be seen on more detail in Figure 5.5. In that same image the system's lack of response to the already know slight up-slight down reference change is shown. The error reaches a maximum of 0.2° for one of the experiments, while it makes it to 0.3° for the other one.

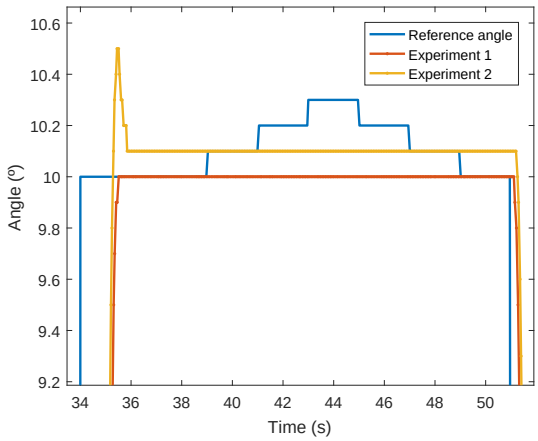

Figure 5.5: Response around 10°

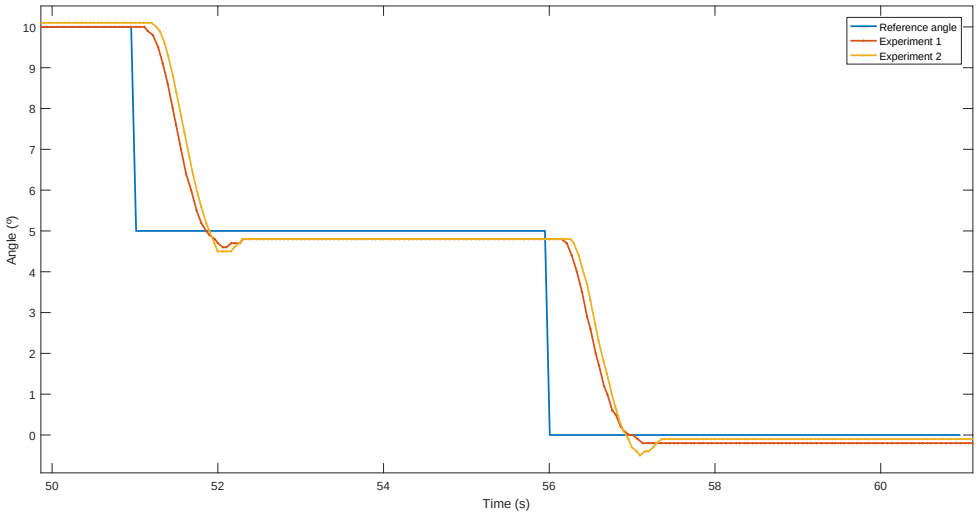

Figure 5.6: Drop from 10° to 5°, to 0°

Figure 5.6 shows who medium drops (of 5° each). On both cases, and both experiments, the system presents overshoot and is not able to reach the desired angle.

5.1.2 Scenario 2

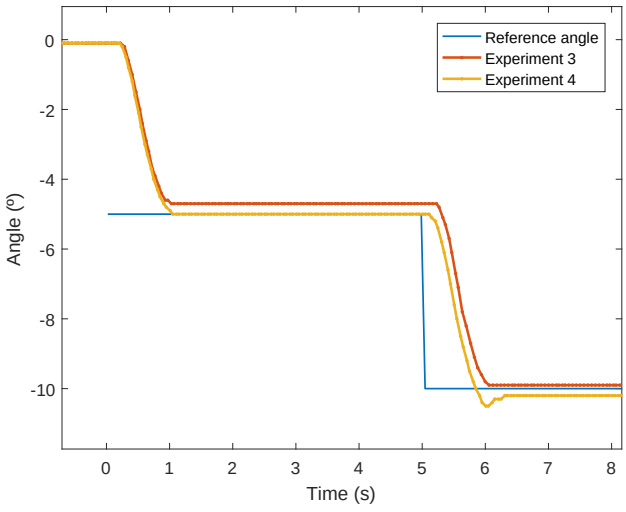

Figure 5.7: Response around 5°

Similar to the first scenario, on the experiments of the second set the vehicle starts with the wheels steered to 0°. At time t=0s, reference angles start being sent. Figure

5.7 shows two medium drops, but the vehicle responds differently to each of them on each experiment. On Experiment 3, the system is unable to reach any of the references. However, on Experiment 4 the system achieves the first desired angle, but overshoots on the second one, stabilizing with an error of 0.2°.

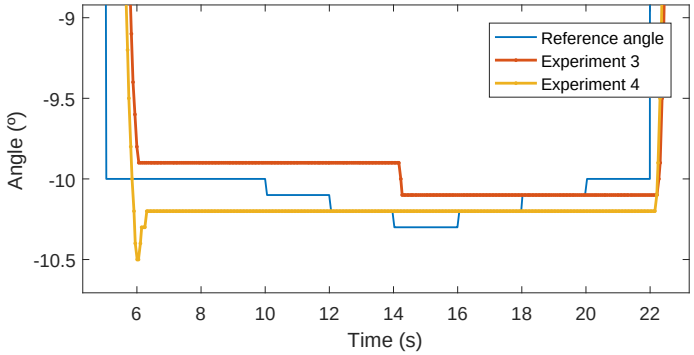

Figure 5.8: Drop from 0° to -5°, to -10°

Following Figure 5.7, Figure 5.8 shows the vehicle's response around -10°, when subjected to slight increase and decrease changes on the reference angle. On this case, both experiments act differently based on where they have ended up from the previous drop. Experiment 3, that has not reached the desired angle, stays on a erroneous value until the error is big enough (0.4°) to make it move, whereas Experiment 4, coming from an overshoot that also does not reach the correct output angle, stays on the same angle because its error remains within±0.3° of the desired one.

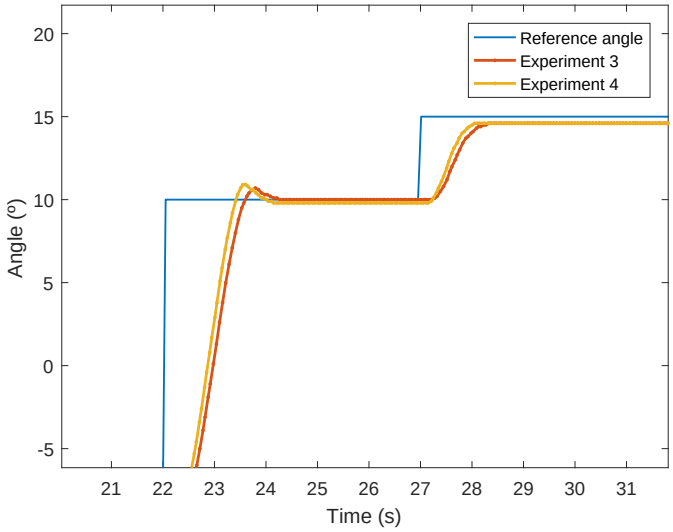

Figure 5.9: Abrupt jump to 10°, medium jump to 15°

Figure 5.9 exemplifies that abrupt increases/decreases lead to overshoot, since this is the case for both experiments when the reference changes on 20°. In this case, only one of the experiments achieves the correct angle. On the other hand, on the medium increase that follows the abrupt one the vehicle does not overshoot, but it also is not able to reach the desired angle on any of the experiments.

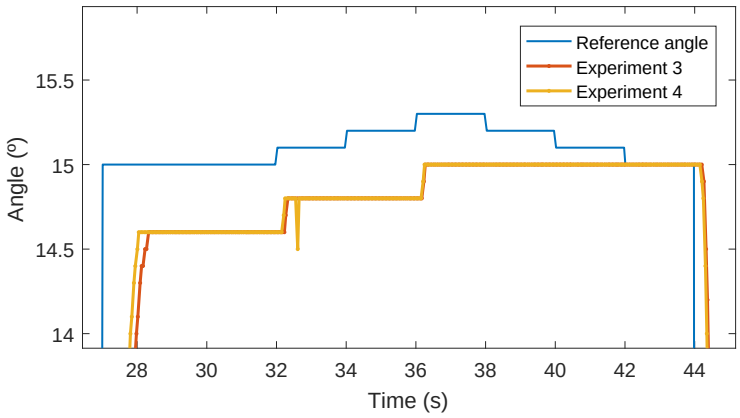

Figure 5.10: Response around 15°

In Figure 5.10 one sees that both experiments behave very similarly, keeping at first an error of 0.4°, which should not happen. However, due to this big difference they respond to the slight increases on the reference, although they do not actually reach it and keep an error. The sudden down peak on Experiment 4 around t=32s might be due to either some irregularity on the ground that forced the wheels to turn for a moment, or more likely is just the consequence of noise on the conversion from analogue to digital signal.

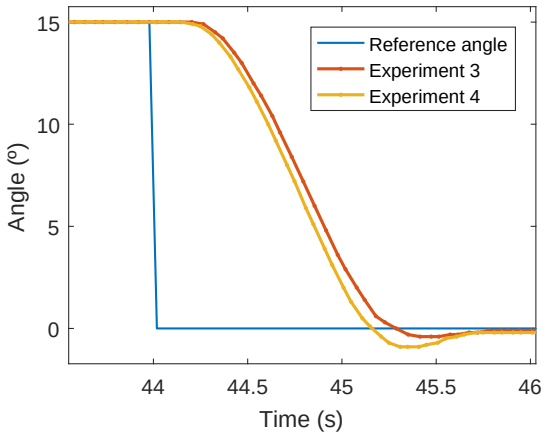

Figure 5.11: Abrupt drop of 15°

Figure 5.11 portrays the last reference change of Scenario 2, which is an abrupt drop and as such, results in an overshoot on both experiments. As the close-up in Figure 5.12 shows, none of the trials reach the desired angle.

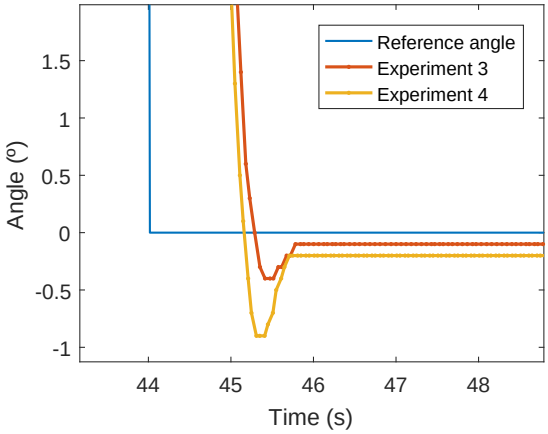

Figure 5.12: Close-up of Figure 5.12

5.1.3 Concluded Remarks

In general, the bare system without any compensator does not follow the reference angle satisfactorily. Sometimes it is due to overshooting, on other occasions it is just unable of reaching the reference. In summary, from these two experiments only in a few of the shifts the vehicle responded in a desirable way, before implementing the new controller.

5.2 Behavior with Compensator Version 1

In this section, the response that the vehicle has once the compensator is implemented is presented. These results are based on the first version of the compensator (v1). The second version of the compensator (v2) is developed from the results of compensator v1, and its results are presented on Section 5.3. Two experiments were made with the implementation of compensator v1, and once again both of them are displayed in the following section.

5.2.1 Scenario 1

Figure 5.13 marks the beginning of the trial. The first reference angle is 5°. In both experiments, the current angle starts to approach the modified one, but it seems that it is

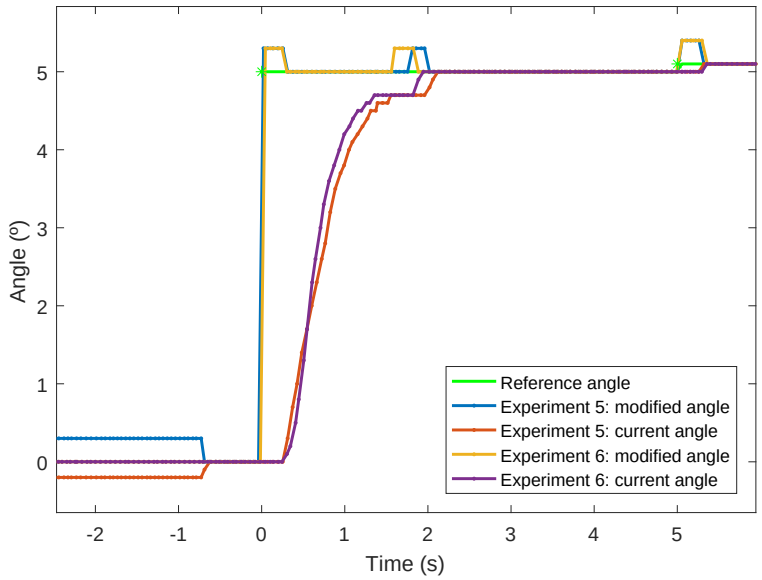

Figure 5.13: Start to 5°

going to stabilize with some error. However, when that starts to happen the compensator comes in, providing a new reference above the desired one and rising the current angle to the correct one. Therefore, the error that would have been there in the absence of compensator is eliminated.

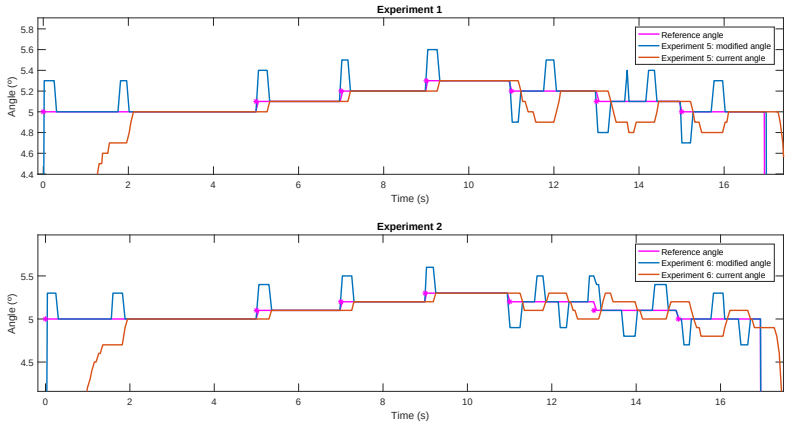

Figure 5.14: Response around 5°

Following from 5.13, 5.14 presents the response of the vehicle when subjected to slight increases and decreases of the reference angle. The graph has been divided in two, separating each experiment, for easier reading. However, it is a continuation from the

previous one. In this case, the response of the system is also satisfactory: the compensator provides the modified reference with enough error to make the vehicle respond, reaching in this manner the references it could not in Figure 5.1

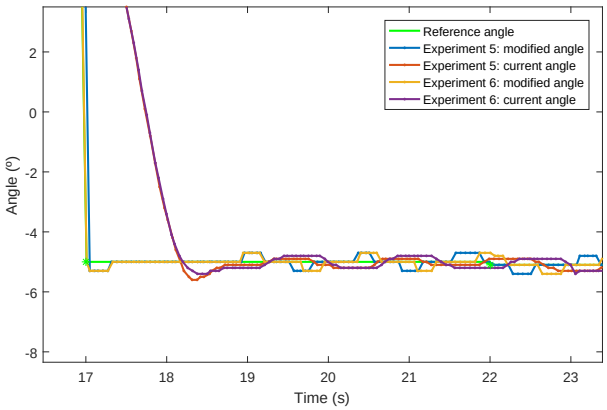

Figure 5.15: Drop from 5° to -5°

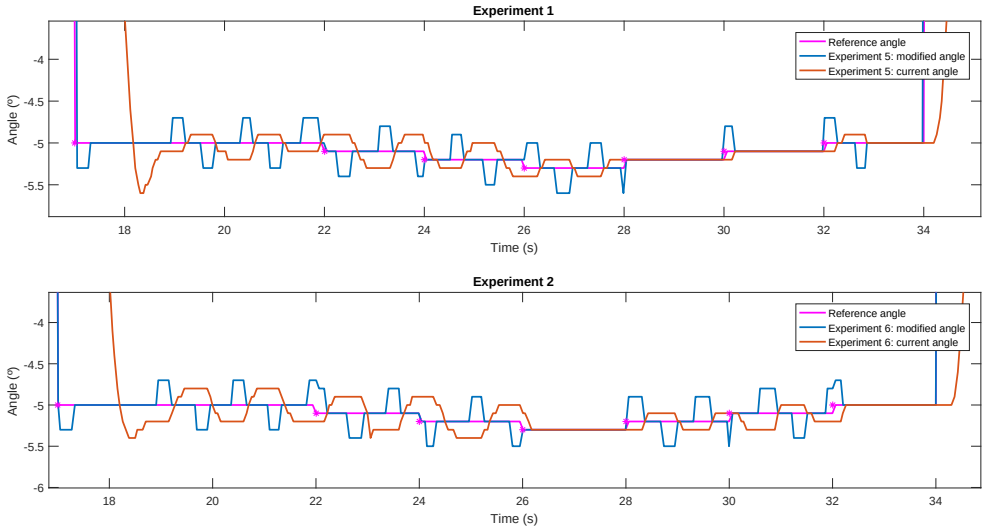

Figure 5.16: Response around -5°

Figures 5.15 and 5.16 show the result of an abrupt drop from 5° to -5° and its following slight decreases and increases. Due to the abruptness of the drop, on both cases there is an overshoot. Then, the compensator provides a modified reference to lift the angle back up, but on doing so the current angle exceeds the desired one. To fix this, the modified reference angle is again below the original one, and at pursuing it the current output angle goes to far. In this manner, the system enters an oscillating, unstable state,

which is perpetuated during the slight decreases, in both experiments. However, when the reference angle starts to increase, Experiment 5 falls into line and takes the desired value, while Experiment 6 keeps on oscillating. This is due to the point of the oscillation in which the reference change happens, and since the vehicle does not respond exactly the same way every time, there is no way of predicting it. All in all, this is not a good result regarding stability.

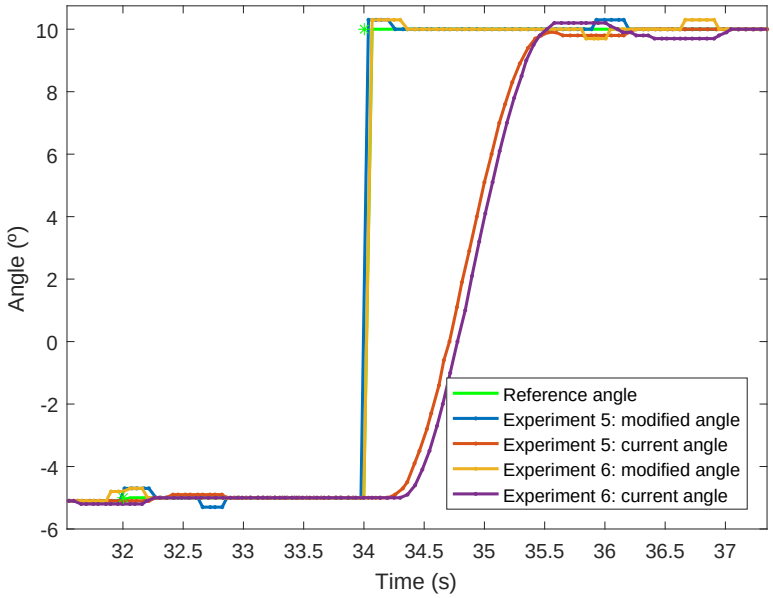

Figure 5.17: Jump from -5° to 10°

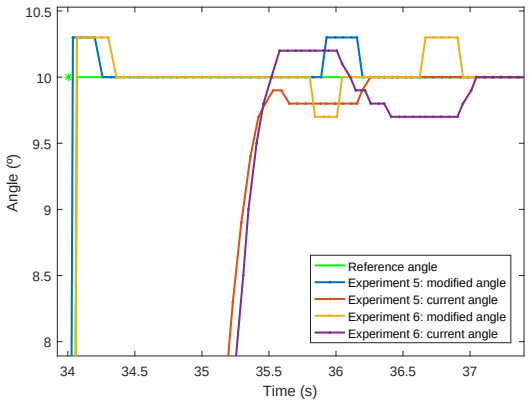

Figure 5.18: Close-up from 5.17

Figure 5.17 and its close-up 5.18 depict the vehicle's response to an abrupt jump. Interestingly enough, only Experiment 6 presents overshoot, that with the modified ref-

erence's help, goes back to the desired angle. On the other hand, Experiment 5 falls short of the original reference, but the modified one pulls it to the correct value. Once again, this is a satisfactory result, because it eliminates the error once it is stable, whereas the lack of compensator situation presented a steady state error.

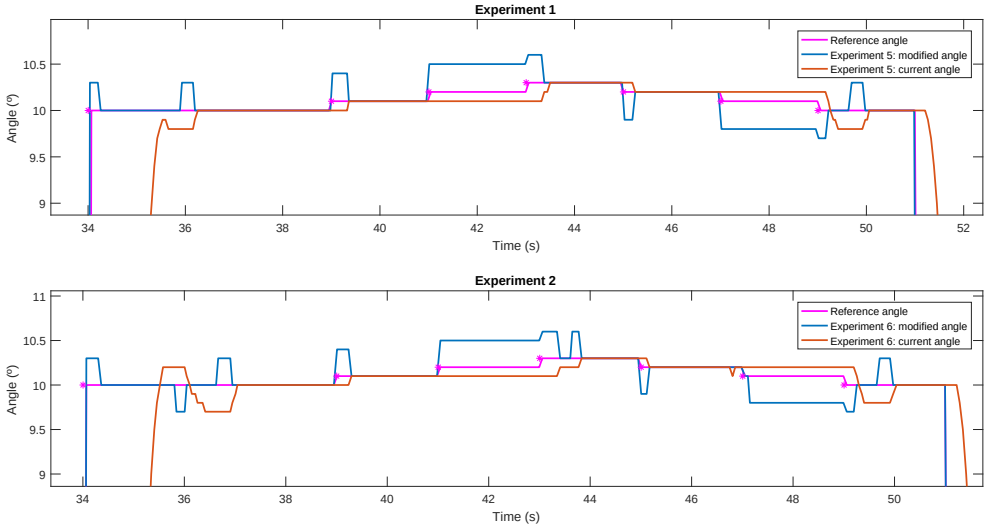

Figure 5.19: Response around 10°

Figure 5.19 presents how the vehicle responds to slight increases and decreases on the area around 10°. Once again, both experiments are separated for easy reading, and in this case both of them show the same behavior. The system is able to follow along the first increment, but when the second step of same height comes, it stays on the same value, even though the modified reference is prompting it to rise. However, on the third step the modified value is even bigger, causing the vehicle to move. The same situation takes place when decreasing these steps.

Figure 5.20 shows a medium drop, from 10° to 5°, to which both experiments answer with overshoot. However, only Experiment 5 achieves the desired angle afterwards, while Experiment 6 enters an oscillatory state. On the case with no compensator, Figure 5.6, none of the experiments achieved a good result. Although it is favorable that the compensator succeeded on at least one of the two experiments, it is not a good enough result to consider it a solution for that situation.

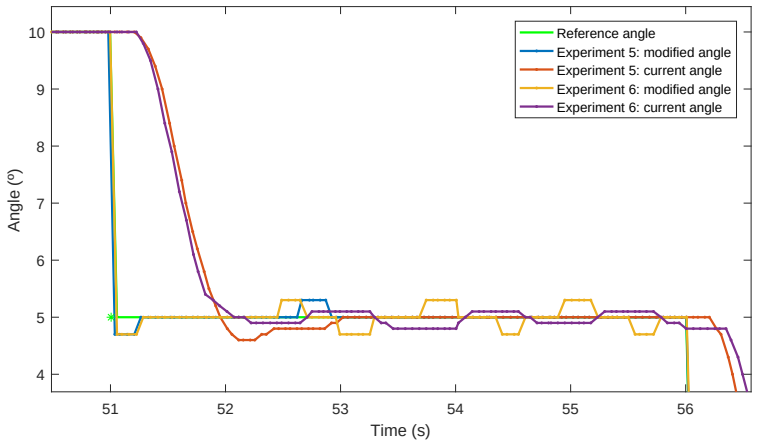

Figure 5.20: Drop from 10° to 5°

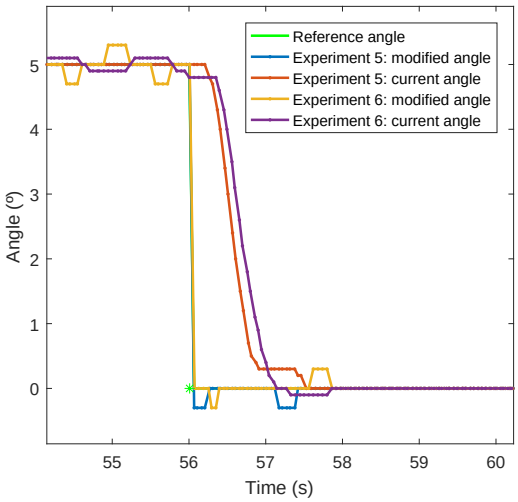

Figure 5.21: Drop from 5° to 0°

The last drop from Scenario 1 depicts satisfactory results on 5.21, because independently of the system being oscillating previously, it achieves the desired angle.

5.2.2 Scenario 2

Figure 5.22 presents two medium angle shifts. Similarly to those on the end of Scenario 1, the first drop (from 0° to -5°) results on oscillation for both experiments, while the second one is successful on achieving the correct angle, even if there is some oscillation.

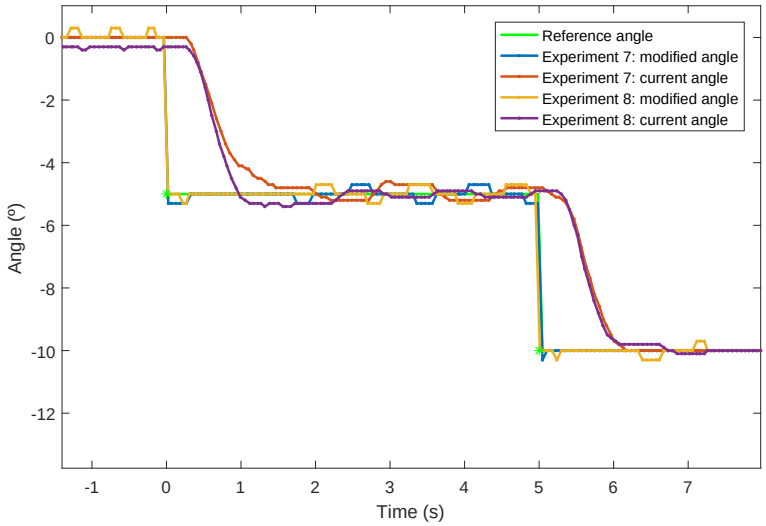

Figure 5.22: Drop from 0° to -5°, to -10°

Figure 5.23 depicts another decrease and increase situation. In this case, in two of the steps, because of the modified reference Experiment 7 goes beyond the desired angle and starts oscillating. On the other hand, Experiment 8 achieves most of the desired values. However, on two occasions the vehicle does not move its wheels even if the error is 0.4°, which should be enough to make it move.

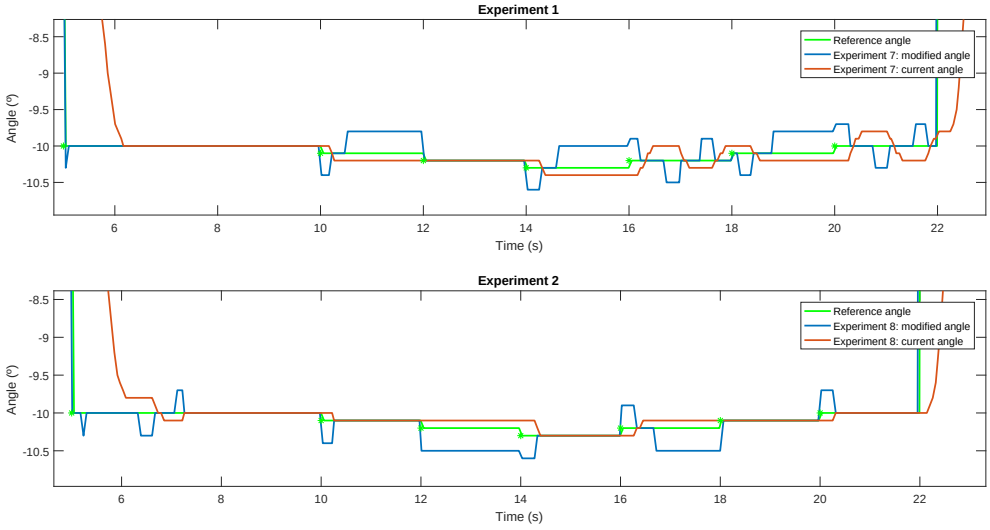

Figure 5.23: Response around -10°

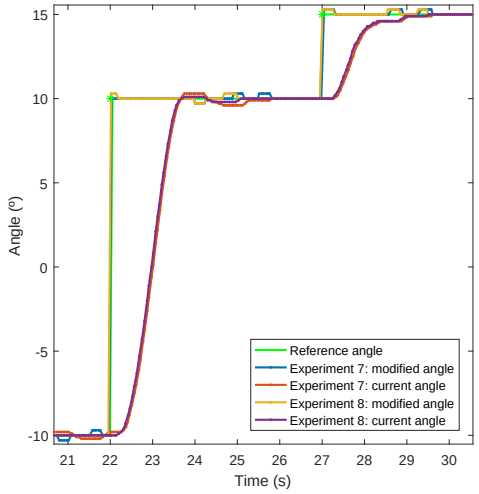

Figure 5.24: Abrupt jump to 10°, medium jump to 15°

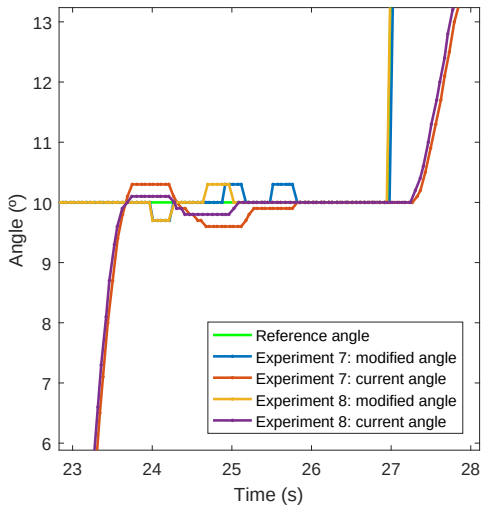

Figure 5.25: Close-up to 5.24

Figures 5.24 and 5.25 present a very abrupt jump, a close-up from its stabilization and a medium jump. The overshoot of the abruptness is counteracted by the compensator, and after a few oscillations both experiments achieve the desired angle. The 5° jump does not overshoot, it actually falls short of the goal, but eventually reaches it due to the modified reference.

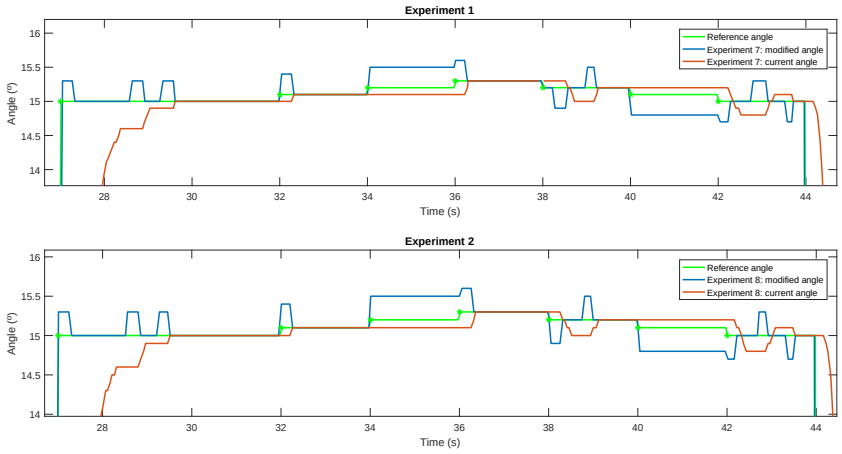

Figure 5.26: Response around 15°

The situation in Figure 5.26 is very similar to that of Figure 5.19: the system achieves the desired result in some of the steps, whereas in others it stays stable even if the error should be enough to make it move. This is a better situation than not having

a compensator at all, however it is not completely reliable because it does not always comply.

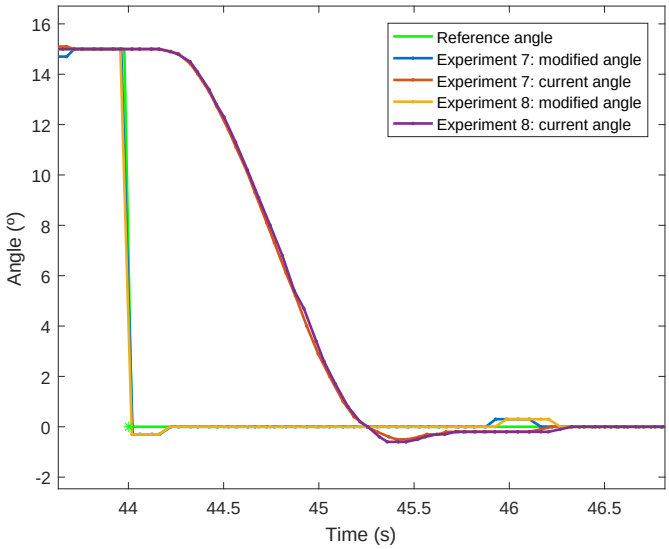

Figure 5.27: Abrupt drop of 15°

As stated in other abrupt reference changes, these result in overshoot, as Figure 5.27 depicts. However, after just a few oscillations and with the help of the compensator, the current angle meets the desired one. This is a satisfactory result.

5.2.3 Concluded Remarks

Without any doubt, the results obtained with the implementation of the compensator are better than those where the system was untouched. Many outputs that otherwise could not have been obtained have been achieved. However, incurring in oscillation is not a good result. In general, it is not desirable to work with unstable systems. However, it is possible that for the specific application of this steering controller, if the oscillation does not provoke a big displacement, it might be acceptable, or at least better than staying on an angle with a big error.

The results from this experiment are going to be used to develop a second version of the compensator's program. It has been observed that the two main problems on these results are: oscillation and lack of movement of the wheels, for errors bigger than 0.3°. The first one occurs on areas closer to the middle. whereas the second one occurs on areas further away. In order to fix this, the proposed approach is to adapt the compensating amount added to the reference, depending on which area the reference is in. Version 2 of the program still follows the same algorithm presented in Figure 3.10, the only variation

being the compensation value added to the reference, depending on what region the reference belongs to. Table 5.1 presents the proposition for the modified compensation amounts (depending on reference) implemented in version 2 of the code.

Table 5.1: Compensation amounts

Reference (°)	**Compensation amount (°)**
$0 \leq \lvert\delta_{reference}\rvert < 3$	0.3
$3 \leq \lvert\delta_{reference}\rvert < 7$	0.2
$7 \leq \lvert\delta_{reference}\rvert < 8$	0.3
$8 \leq \lvert\delta_{reference}\rvert$	0.4

5.3 Behavior with Compensator Version 2

This section presents the results of the experimental work done under the implementation of the compensator v2. Since the experiments have only been performed once for each scenario, the data from the experiments without any compensator have been added to the plots, for comparison.

5.3.1 Scenario 1

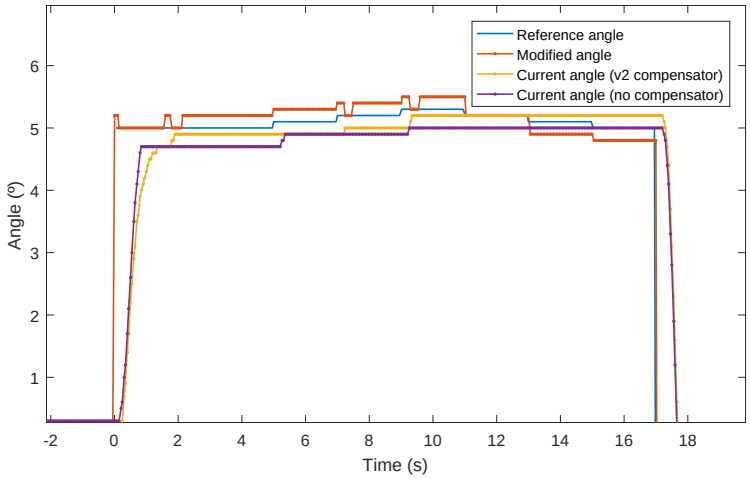

Figure 5.28: Start to 5°

The first reference value of the experiment is 5°. As Figure 5.28 presents, the vehicle equipped with compensator v2 is unable of reaching that value. This is due to the fact

that the modified reference is not enough to rise the current angle to the desired value, because the error with respect to the modified reference is 0.3°, which is within the area where the motor will not move. However, the steady state error with respect to the desired angle is only 0.1°, which is better than that of the system without any compensator. A similar response takes place when the reference moves slightly up and down.

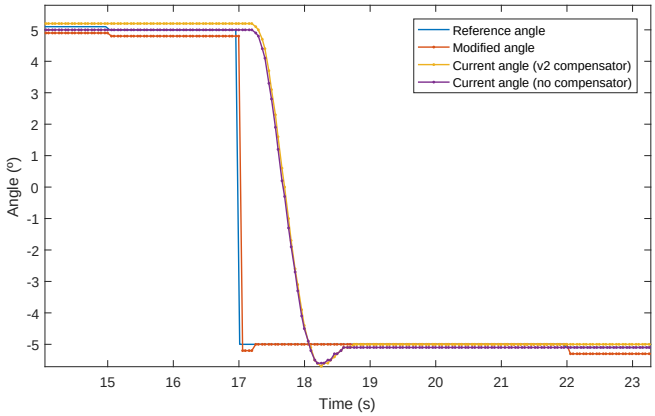

Figure 5.29: Drop from 5° to -5°

Figure 5.29 shows an abrupt drop to -5°. As expected, the system overshoots in both cases (with and without compensator), but on the lack of a controller the system does not reach the desired output, while it does once a compensator is implemented.

Figure 5.30 presents the response around -5°, when the reference increases and decreases. Similarly to Figure 5.28, the modified reference is not enough to cause the system to follow the reference accurately, so in this case the compensator does not bring a big benefit above the bare system (without compensator). Following, Figure 5.31 depicts an abrupt jump, answered with overshoot by the vehicle on both cases. Once again, the compensator helps the UGV to reach the adequate steering angle, while the bare system is unable to do so.

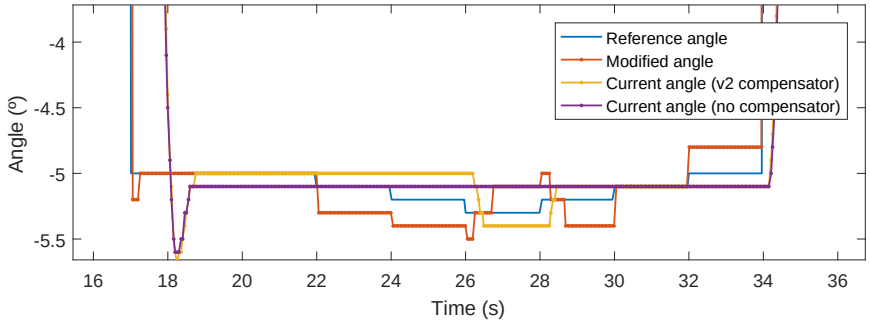

Figure 5.30: Response around -5°

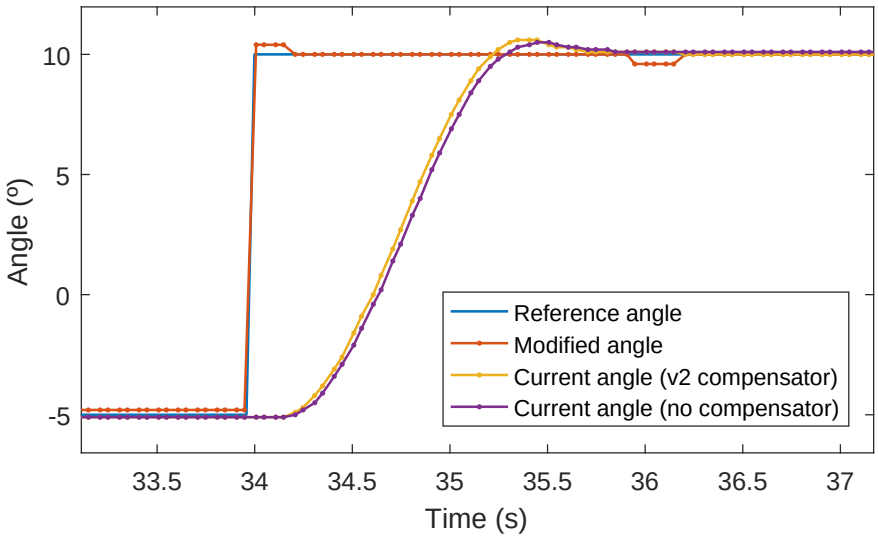

Figure 5.31: Jump from -5° to 10°

After the jump to 10°, the response around that point is studied. In this case, because the compensation amount has been increased for this region, the vehicle is able to reach the reference in some of the point (unlike the system without compensator, which stays constant throughout the whole increase/decrease). However, there are some steps there the excessive compensation causes the vehicle's output to oscillate as Figure 5.32 depicts.

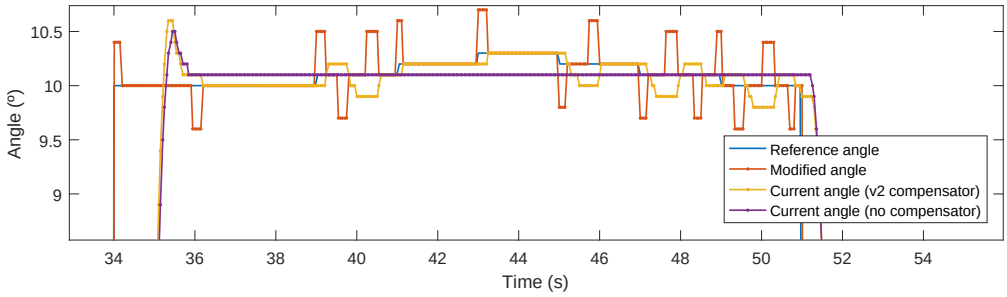

Figure 5.32: Response around 10°

Figure 5.33 presents two 5° drops with different behaviors. Both of them have a certain overshoot, and the system without compensator does not achieve the desired angle in neither. However, the compensator v2 causes the vehicle to follow the reference angle only on the area around 0°, while the compensation amount around 5° is not enough. This concludes the behavior of compensation v2 in Scenario 1.

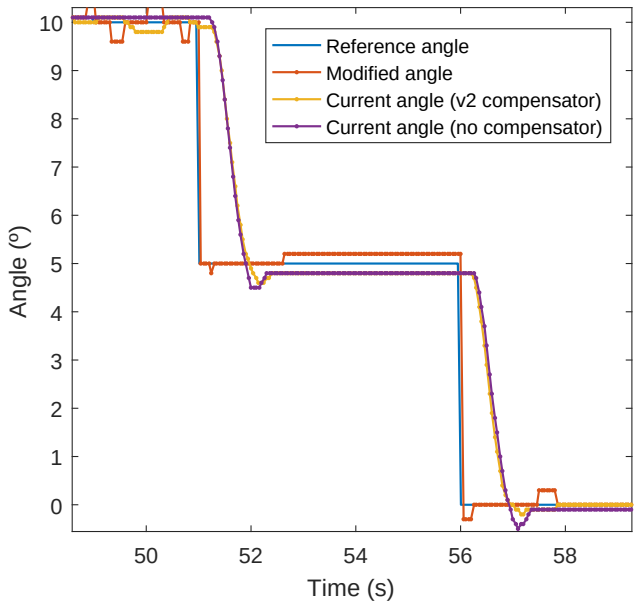

Figure 5.33: Drop from 10° to 5°, to 0°

5.3.2 Scenario 2

The first shifts in Scenario 2 are two 5° drops, shown in Figure 5.34. The first one is smoothly followed by the vehicle, both with and without compensator, whereas the second drop is not successful in any of the experiments: when there is no compensator, the vehicle stays on a fixed value, not following the changes; version 2 of the compensator causes the system to oscillate, due to its excessive compensation amount. This oscillation is perpetuated during the study around -10°, see Figure 5.35.

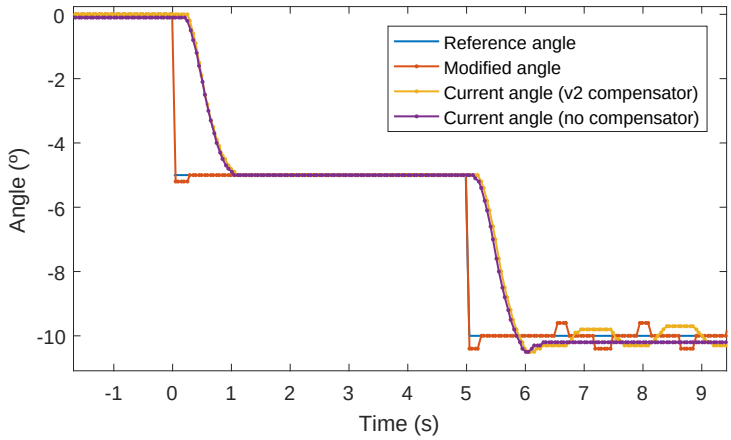

Figure 5.34: Drop from 0° to -5°, to -10°

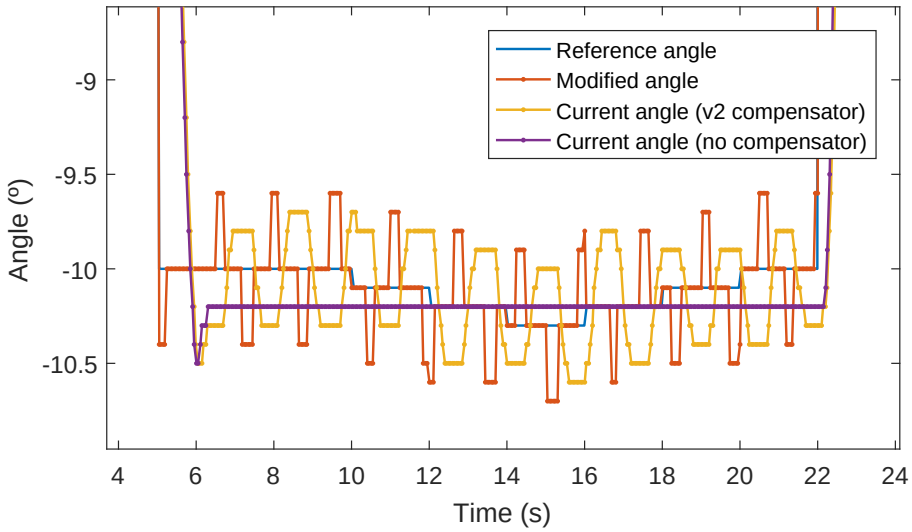

Figure 5.35: Response around -10°

Figure 5.36 depicts an abrupt and a medium jump. The compensator succeeds in both of the,, while the bare system does not achieve the desired angle in neither. This leads to the situation shown in Figure 5.37: the system with the compensator responds well during the increase, but starts oscillating during the decrease of the reference. Meanwhile, the bare system does not follow the reference properly.

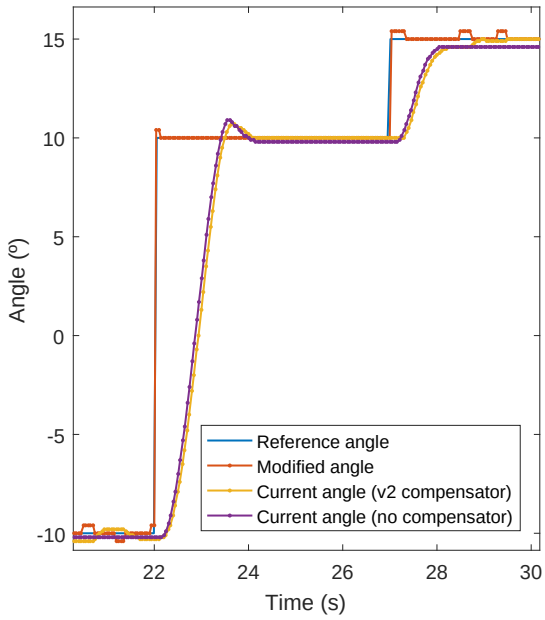

Figure 5.36: Abrupt jump to 10°, medium jump to 15°

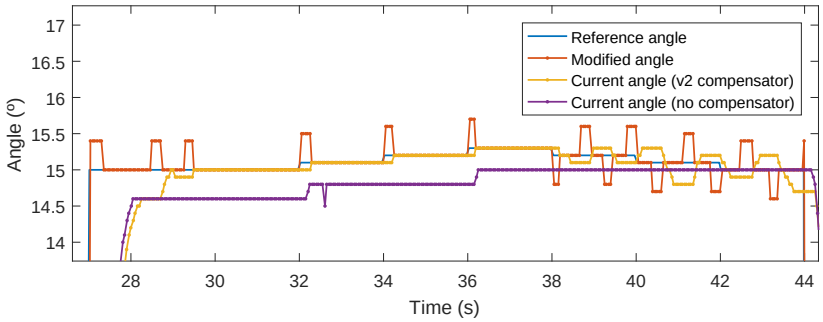

Figure 5.37: Response around 15°

The experiment concludes with an abrupt drop from 15 to 0, see Figure 5.38. The vehicle with compensator responds well to the overshoot, while the system without it does not achieve the desired reference angle.

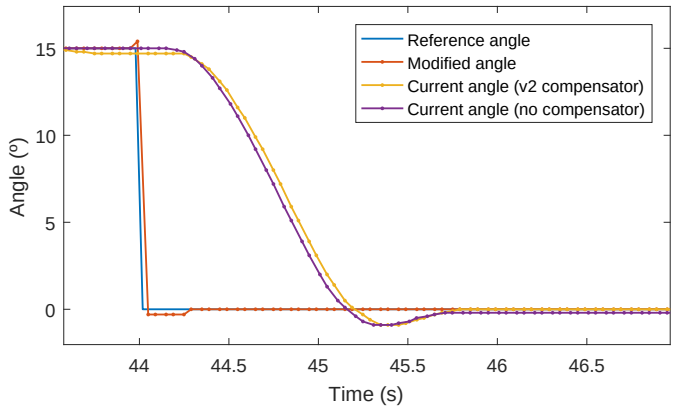

Figure 5.38: Abrupt drop of 15°

5.3.3 Concluded Remarks

It was expected for version 2 of the compensator to perform better than version 1. However, the results have not shown this. While on some occasions the system responds properly, other times the compensation amount is not enough, and the vehicle does not reach the desired angle. In addition, the problem of oscillation still takes place. Nevertheless, the results obtained by version 2 of the code are still better than the results without any compensator.

5.4 Error Comparison

The analysis of the plots resulting from the collected data only provides a qualitative perspective from the results. In order to quantify the impact of the designed controller some metrics must be set. In this case, since the goal was to eliminate the steering angle error, this will be the measurement.

The error is computed as stated earlier in equation 3.10. However, the relevant measurement of the error for the experiments of this thesis are the mean error and the mean absolute error, calculated as equations 5.1 and 5.2 show.

$$\text{Mean error} = \frac{1}{n}\sum_{i=1}^{n} e_i \tag{5.1}$$

$$\text{Mean absolute error} = \frac{1}{n}\sum_{i=1}^{n} |e_i| \tag{5.2}$$

With the help of Matlab, the error for each value of current steering angle is computed (only for the time where there is a reference angle). Then, a Matlab function computed the mean error and the mean absolute error. This is done for every experiment. In the end, the mean and mean absolute errors of vehicle without compensator, with compensator v1, and with compensator v2 are available for comparison and drawing conclusions.

Tables 5.2 and 5.3 present the mean error and mean absolute error of the experiments in Scenarios 1 and 2. The goal is to have the mean and mean absolute error values as close to zero as possible. Therefore, the tables show that the best results have been obtained from the implementation of compensator version 1. In addition to that, in both scenarios the worst results have been the ones of the experiments without any compensator. This proves the effectiveness of the added controller.

Table 5.2: Errors of Scenario 1

	No compensator		**Compensator Version 1**		**Compensator Version 2**
Experiment #	*1*	*2*	*5*	*6*	*9*
Mean error	-0.1851	-0.1199	-0.0832	-0.0528	-0.0694
Mean absolute error	0.6080	0.5632	0.5278	0.5544	0.5296

Table 5.3: Errors of Scenario 2

	No compensator		**Compensator Version 1**		**Compensator Version 2**
Experiment #	*3*	*4*	*7*	*8*	*10*
Mean error	-0.1165	-0.2176	-0.1022	-0.1228	-0.1157
Mean absolute error	0.9376	0.8839	0.8268	0.8954	0.8585

It must be noted that the mean error takes a much smaller value than the mean absolute error. This is due to errors of opposite signs canceling each other out when computing the mean. This is why the mean is not a good measurement of the system achieving the desired angle; there could be a case where the system was oscillating a lot, but the mean was 0, because the oscillations were symmetrical to the reference (e.g. the mean of the $sin(x)$ function is 0, but that does not mean that its error with respect to the x axis is always 0). Nevertheless, the computation of the mean error provides information regarding the symmetry of the error. If it is close to 0, as in the case of the compensators, it means that the error is distributed in a reasonably symmetrical manner.

In order to obtain information about the system's ability to follow the reference, without being influenced by the sign of the error, the mean absolute error is computed. Once again, the best results have been obtained under the implementation of the compensators, version 1 being better than version 2. In this case, the mean absolute error has such a high value (around 0.8°) because the error during transitions is also taken into account for the computation.

Chapter 6

Conclusions and Future Work

The goal of this thesis is to develop a steering controller for an iCab UGV. Due to the system specifics of the testing vehicle, in which the PID controller of the low level control could not be modified, the control had to be implemented externally.

The first approach to solving the problem at hand consisted of modeling the system and designing an external PID. However, this approach had to be discarded due to the lack of similarity between the Ackerman steering geometry and the actual mechanical structure of the vehicle, as well as the difficulty to perform measurements of the UGV's mechanism.

The second approach to controlling the steering angle was to design a deadband compensator. It was selected based on the steady state error resulted from the internal steering controller of $\pm 0.3°$. Based on this, a compensator was developed in C++ and implemented through ROS-based architecture. Based on the results from the experimental work of this controller, a second version of the code was developed.

The vehicle for testing the controller was a research platform known as iCab. A total of 10 experiments were carried out on 2 different scenarios. The behavior of the vehicle prior to having the external controller, the behavior with the implementation of the compensator's version 1 and the behavior with the implementation of the compensator's version 2 were characterized.

The results of the experiments showed that both versions of the compensator brought an improvement in the mean error and mean absolute error of the experiments' measurements. However, the results have not been as quantitatively significant as the qualitative analysis suggested. This might be due to the fact that the mean error and mean absolute error are calculated from each reading of the current steering angle (with respect to the reference) of the experiments. This means that the error during transitions, before stabilization is drawn into the computation. Therefore this is not a measure of the steady state error, which would probably depict a more significant improvement.

Future work on this topic could expand and refine the compensators developed in this thesis. Upon studying of the irregular behavior of the system, a more complex

code may be developed, refined for different turns (more abrupt or slighter changes on the reference angle). Additionally, since one of the main problems of the compensated system is oscillation, a "oscillation detector" may be developed, which would stop sending a modified reference if this is causing the vehicle to oscillate.

Another possibility regarding further research in this topic would be to search for a different, applicable model in the literature, and approximating parameters that might result difficult to measure.

In any case, in order to measure the effectiveness of any developed solution, it would be essential to obtain the odometry data of the controller's performance: collecting the data from the wheels encoder odometry and another reliable odometry form (Velodyne lidar sensor, for example), in order to check if the accuracy of the steering has improved.

Appendix

Appendix A

Lists

ADAS Advanced Driver Assistance Systems

ABS Antiblock Brake System

iCab Intelligent Campus Automobile

LSI Laboratorio de Sistemas Inteligentes

MPC Model Predictive Control

PID proportional-integral-derivative

ROS Robot Operating System

UGV Unmaned Ground Vehicle

List of Figures

1.1 Steering angle of a turning vehicle 4

2.1 Example of the substitution of classically mechanical linkages for an electronic system on Steer-by-Wire [2] 8
2.2 Past and potential future evolution [4] 9

3.1 Comparison of Velodyne and wheel encoder odometries on different path geometries 11
3.2 Graphical model for wheel odometry [13] 13
3.3 Control architecture on UGV 13
3.4 Original control scheme on UGV 14
3.5 Proposed control scheme on UGV 14
3.6 Ackerman model 15
3.7 Control scheme including compensator 17
3.8 Position error explanation 17
3.9 Expected behavior after implementing the compensator 18
3.10 Algorithm of the compensator 19

4.1 The testing vehicle, iCab1 21
4.2 Motor-encoder system on iCab1 22
4.3 Sign convention of steering angles 23
4.4 Reference angle sequence for the experiments 23
4.5 Scenario 1: plot of reference angles 24
4.6 Scenario 2: plot of reference angles 24

5.1 Response around 5° 27

5.2 Drop from 5° to -5° 28
5.3 Response around -5° 28
5.4 Jump from -5° to 10° 29
5.5 Response around 10° 29
5.6 Drop from 10° to 5°, to 0° 30
5.7 Response around 5° 30
5.8 Drop from 0° to -5°, to -10° 31
5.9 Abrupt jump to 10°, medium jump to 15° 31
5.10 Response around 15° 32
5.11 Abrupt drop of 15° 32
5.12 Close-up of Figure 5.12 33
5.13 Start to 5° 34
5.14 Response around 5° 34
5.15 Drop from 5° to -5° 35
5.16 Response around -5° 35
5.17 Jump from -5° to 10° 36
5.18 Close-up from 5.17 36
5.19 Response around 10° 37
5.20 Drop from 10° to 5° 38
5.21 Drop from 5° to 0° 38
5.22 Drop from 0° to -5°, to -10° 39
5.23 Response around -10° 39
5.24 Abrupt jump to 10°, medium jump to 15° 40
5.25 Close-up to 5.24 40
5.26 Response around 15° 40
5.27 Abrupt drop of 15° 41
5.28 Start to 5° 42
5.29 Drop from 5° to -5° 43
5.30 Response around -5° 43
5.31 Jump from -5° to 10° 44
5.32 Response around 10° 44

5.33 Drop from 10° to 5°, to 0° 45
5.34 Drop from 0° to -5°, to -10° 45
5.35 Response around -10° 46
5.36 Abrupt jump to 10°, medium jump to 15° 46
5.37 Response around 15° 47
5.38 Abrupt drop of 15° 47

C.1 Gantt diagram of the workload distribution 61

D.1 Mechanical link: initial position 62
D.2 Mechanical link: position after turning 63

List of Tables

3.1 Nomenclature of dimensions 15
3.2 Selection of parameters for the compensator 20

4.1 List of angles and durations on each scenario 24

5.1 Compensation amounts 42
5.2 Errors of Scenario 1 48
5.3 Errors of Scenario 2 49

C.1 Budget estimate 61

Appendix B

Legislation Framework

This appendix deals with the legal framework for autonomous vehicle testing in Spain. On 23rd December 1998, the *Real Decreto 2822/1998* law was passed, in which the Dirección General de Tráfico (DGT) entity was bestowed the power to grant special authorization to manufacturers, second-phase manufacturers and official laboratories for holding extraordinary tests with research purposes.

However, due to the technological improvements that no longer were covered by the aforementioned law, and with the aim of contributing to safety, sustainability, automotive industry and research, DGT presented a modification of the law on 2015, *Instrucción 15/V-113*. Said instruction deals with the conditionsa vehicle must fulfill in order to apply and the reach of the authorization: an extent of 2 years, only valid for national territory, etc. In addition, the possibility to apply is granted to more organizations than the original law stated: *"...podrán solicitar la autorización para la realización de pruebas y ensayos: los fabricantes de los vehículos autónomos, sus fabricantes de segunda fase y los laboratorios oficiales. Sin perjuicio de lo anterior, y por analogía, se entenderán legitimados así mismo para su solicitud, los fabricantes o instaladores de la tecnología que permite al vehículo plena autonomía, las universidades y consorcios que participen en proyectos de investigación en los términos descritos en la presente instrucción."* This means "[the following] will be able to request authorization to carry out tests and trials: autonomous vehicle manufacturers, their second-phase manufacturers and official laboratories. Without prejudice to the foregoing, and by analogy, the following shall also have legitimacy: the manufacturers or instalers of the technology of the vehicle that allows it full autonomy, universities and consortia participating on research projects, on the terms described on this instruction".

Appendix C

Social Economic Aspect

This thesis has contributed to the steering control of the iCabs of the LSI, but it is only a small part of a larger project, because a lot more of work and research has been put by the researchers of the LSI to achieve autonomous functioning. Once the iCabs are working, they will not have a big impact in any area: regarding economics, they are not going to be commercialized, therefore will not bring economic benefits to the University. They will not have a significant ecological impact, neither for good nor for bad, because they do not run on fuel and will not be emitting pollution, but they do not provide advancements or improvements on ecologism. The use intended for these autonomous vehicles is to transport visitors within campus vicinity. Therefore, it is possible to say that the implementation is quite local and will have no social significance.

C.1 Budget

The economical cost of the elaboration of this thesis has 3 main expenses: the purchase of the hardware needed as a research platform, the software needed for dealing with the collected data from the experiments, and finally the manpower put in by the author for the realization of the thesis.

The research platform is comprised by an electrical golf cart, commercialized under the name of E-Z-GO; a Velodyne; a camera; many other minor sensors and actuators installed by the research staff, as a modification of the original cart.

The software used for managing the data has been MATLAB R2016b - academic use. The university provides a license for all the students and staff, so in this case it was not particularly purchased for the sole use of this thesis. However, for budget considerations as an independent project, the cost of said license will be considered.

Finally, the hours invested by the author of the thesis, which has had a duration of 4.5 months, mounting a workload of 20h per week, add to a total of 360h. The laboring cost is estimated at 6€/h.

Table C.1: Budget estimate

Concept	**Units**	**Cost**
E-Z-Go cart	1	2000€
Velodyne	1	8000€
Camera	1	3000€
Other sensors	-	2000€
MatLab license (Academic-Individual)	1	500€
Manpower	360h	2160€
Total		17660€

C.2 Thesis process

The Gantt diagram shown in Figure C.1 presents the distribution of the workload of this thesis.

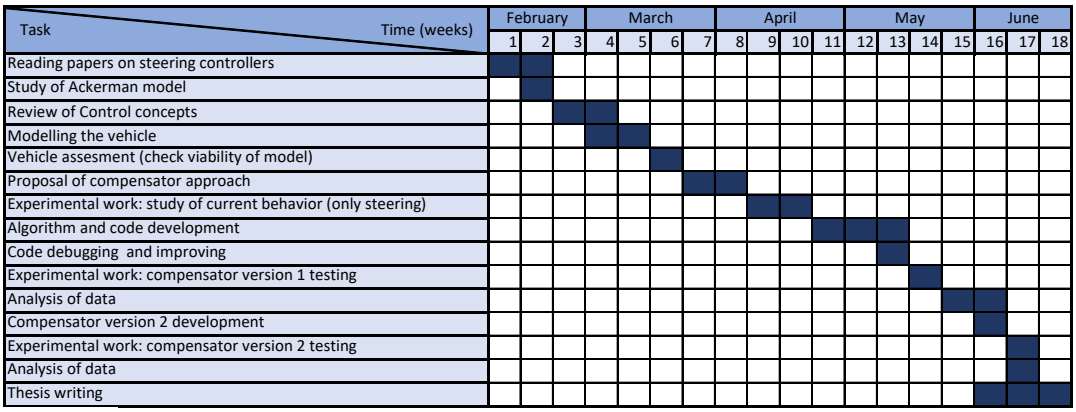

Figure C.1: Gantt diagram of the workload distribution

Appendix D

Model

This appendix presents the mathematical relation between the steering angle of the vehicle and the movement of the mechanical links within it. The mathematical model is based on the Ackerman steering geometry. The goal is to relate the angle of each wheel to the angle of the mechanical link represented in green in Figure 3.6. To do this, the shaft is substituted by a vector, and its two ends receive the name of points P and Q, as seen in Figures D.1 and D.2.

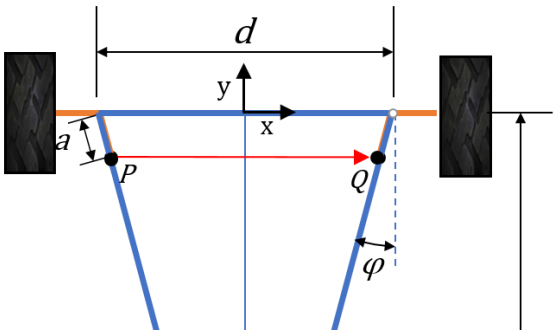

Figure D.1: Mechanical link: initial position

The vector before turning is $\vec{x}_{initial}$, and the vector after the turn is $\vec{x}_{final}$. At finding the angle between these two vectors, we will find the angle that the mechanical shaft has turned. Since the vector has the points P and Q as starting and ending points, we can calculate the vectors as equations D.1 and D.2 show:

$$\vec{x}_{initial} = Q_{initial} - P_{initial} \tag{D.1}$$

$$\vec{x}_{final} = Q_{final} - P_{final} \tag{D.2}$$

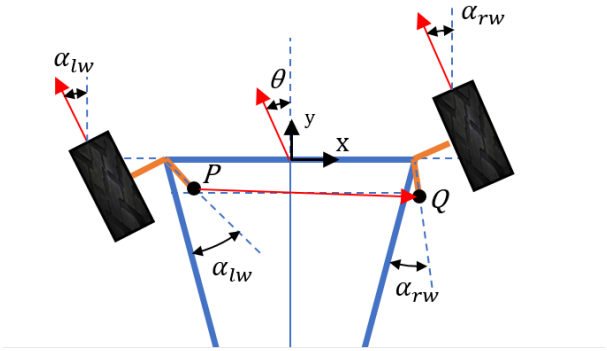

Figure D.2: Mechanical link: position after turning

The origin of coordinates is in the center of the front axle. From Figures D.1 one deducts:

$$P_{initial} = \left(a \cdot \sin\varphi - \frac{d}{2}, -a \cdot \cos\varphi\right) \tag{D.3}$$

$$Q_{initial} = \left(-a \cdot \sin\varphi + \frac{d}{2}, -a \cdot \cos\varphi\right) \tag{D.4}$$

Operating equation D.4 minus D.3 the result is:

$$\vec{x}_{initial} = (-a \cdot \sin\varphi + \frac{d}{2} - a \cdot \sin\varphi + \frac{d}{2}, -a \cdot \cos\varphi + a \cdot \cos\varphi) = (d - 2a \cdot \sin\varphi, 0) \tag{D.5}$$

From Figure D.2 one deducts:

$$P_{final} = \left(a \cdot \sin\left(\varphi + \alpha_{lw}\right) - \frac{d}{2}, -a \cdot \cos\left(\varphi + \alpha_{lw}\right)\right) \tag{D.6}$$

$$Q_{final} = \left(-a \cdot \sin\left(\varphi - \alpha_{rw}\right) + \frac{d}{2}, -a \cdot \cos\left(\varphi - \alpha_{rw}\right)\right) \tag{D.7}$$

Substituting D.7 and D.6 in D.2:

$$\vec{x}_{final} = (d - a\sin(\varphi - \alpha_{rw}) - a\sin(\varphi + \alpha_{lw}), a\cos(\varphi + \alpha_{lw}) - a\cos(\varphi - \alpha_{rw})) \tag{D.8}$$

The angle δ between two vectors $\vec{u}$ and $\vec{v}$ is calculated according to equation (D.9)

$$\cos(\delta) = \frac{\vec{u} \cdot \vec{v}}{\|\vec{u}\| \cdot \|\vec{v}\|} \tag{D.9}$$

Therefore, in this case, the angle γ between vectors $\vec{x}_{final}$ and $\vec{x}_{initial}$ is given by equation (D.10)

$$\gamma = \arccos\left(\frac{\vec{x}_{initial}\vec{x}_{final}}{\|\vec{x}_{initial}\| \ \|\vec{x}_{final}\|}\right) \tag{D.10}$$

From D.5 and D.8:

$$\vec{x}_{initial}\vec{x}_{final} = 2a^2 \sin\varphi(\sin(\varphi - \alpha_r) + \sin(\varphi + \alpha_l)) \tag{D.11}$$

The moduli of the vectors are given by (D.12) and (D.13):

$$\|\vec{x}_{initial}\| = d - 2a\sin\varphi \tag{D.12}$$

$$\|\vec{x}_{final}\| = d^2 - 2ad(\sin(\varphi - \alpha_{rw}) + \sin(\varphi + \alpha_{lw})) + 2a^2(1 - \cos(2\varphi + \alpha_{lw} - \alpha_{rw})) \tag{D.13}$$

If (D.11), (D.12) and (D.13) are subsituted in D.10, the angle γ is solved. This way, γ will only depend on the geometrical parameters of the model.

References

[1] CBInsights. (2017, May) 44 corporations working on autonomous vehicles. [Online]. Available: https://www.cbinsights.com/blog/autonomous-driverless-vehicles-corporations-list/

[2] A. Sharma, "The steering model," *Scribd*, 2002.

[3] H. Wang, Z. Man, W. Shen, Z. Cao, J. Zheng, J. Jin, and D. M. Tuan, "Robust control for steer-by-wire systems with partially known dynamics," *IEEE Transactions on Industrial Informatics*, vol. 10, no. 4, pp. 2003–2015, nov 2014.

[4] K. Bengler, K. Dietmayer, B. Frber, M. Maurer, C. Stiller, and H. Winner, "Three decades of driver assistance systems," *IEEE Intelligent transportation systems magazine*, Oct. 2014.

[5] A. K. G. Balagh, F. Naderkhani, and V. Makis, "Highway accident modeling and forecasting in winter," *Transportation Research Part A: Policy and Practice*, vol. 59, pp. 384–396, jan 2014.

[6] J. Guo, P. Hu, and RongbenWang, "Nonlinear coordinated steering and braking control of vision-based autonomous vehicles in emergency obstacle avoidance," *IEEE Transactions on Intelligent Transportation Systems*, vol. 17, no. 11, Nov. 2016.

[7] C. of the European Communities, "Proposal for a directive of the european parliament and of the council relating to the protection of pedestrians and other vulnerable road users in the event of a collision with a motor vehicle and amending directive 70/156/eec," Feb. 2003.

[8] M. Park, S. Lee, and W. Han, "Development of steering control system for autonomous vehicle using geometry-based path tracking algorithm," *ETRI Journal*, vol. 37, no. 3, pp. 617–625, 2015.

[9] M. T. Emirler, E. M. C. Uygan, B. A. Gven, and L. Gven, "Robust pid steering control in parameter space for highly automated driving," *International Journal of Vehicular Technology*, vol. 2014, Feb. 2014.

[10] J. P. Rastelli, V. Milanes, and E. Onieva, "Cascade architecture for lateral control in autonomous vehicles," *IEEE Transactions on Intelligent Transportation Systems,*, vol. 12, no. 1, Mar. 2011.

[11] R. C. Rafaila, G. Livint, F. of Electrical, Engineering, Applied, I. Faculty, of Electrical, Engineering, Applied, and Informatics, "H-infinity control of automatic vehicle steering," "Gheorghe Asachi" Technical University Iasi, Romania, Tech. Rep., 2016.

[12] X. Du, K. Kiong, Tan, , D. of ElectricalComputer Engineering, and N. U. of Singapore, "Autonomous vehicle velocity and steering control through nonlinear model predictive control scheme," in *2016 1IE -E4E, 2T0ra1n6s, portation Electrification Conference and Expo, Asia-Pacific (ITEC) June Busan, Korea.* IEEE, 2016.

[13] A. Hussein, P. Marin-Plaza, D. Martin, A. de la Escalera, and J. M. Armingol, "Autonomous off-road navigation using stereo-vision and laser-rangefinder fusion for outdoor obstacles detection," *IEEE Intelligent Vehicles Symposium (IV)*, pp. 104–109, 2016.

[14] R. Ackermann, *Observations on Ackermann's Patent Moveable Axles: For Four Wheeled Carriages, Containing Engraved Elevations of Carriages, with Plans and Sections, Conveying Accurate Ideas of this Superior Improvement.* R. Ackermann, 1819. [Online]. Available: https://books.google.es/books?id=Kbg5AQAAMAAJ